


RESEARCH ARTICLE

Open Access



Wheat inositol pyrophosphate kinase TaVIH2-3B modulates cell-wall composition and drought tolerance in Arabidopsis

Anuj Shukla^{1,2†}, Mandeep Kaur^{1†}, Swati Kanwar¹, Gazaldeep Kaur¹, Shivani Sharma¹, Shubhra Ganguli^{3,4}, Vandana Kumari¹, Koushik Mazumder¹, Pratima Pandey⁵, Hatem Rouached^{6,7}, Vikas Rishi¹, Rashna Bhandari³ and Ajay Kumar Pandey^{1*} 

Abstract

Background: Inositol pyrophosphates (PP-InsPs) are high-energy derivatives of inositol, involved in different signalling and regulatory responses of eukaryotic cells. Distinct PP-InsPs species are characterized by the presence of phosphate at a variable number of the 6-carbon inositol ring backbone, and two distinct classes of inositol phosphate kinases responsible for their synthesis have been identified in Arabidopsis, namely ITPKinase (inositol 1,3,4 trisphosphate 5/6 kinase) and PP-IP5Kinase (diphosphoinositol pentakisphosphate kinases). Plant PP-IP5Ks are capable of synthesizing InsP₈ and were previously shown to control defense against pathogens and phosphate response signals. However, other potential roles of plant PP-IP5Ks, especially towards abiotic stress, remain poorly understood.

Results: Here, we characterized the physiological functions of two *Triticum aestivum* L. (hexaploid wheat) PPIP5K homologs, TaVIH1 and TaVIH2. We demonstrate that wheat VIH proteins can utilize InsP₇ as the substrate to produce InsP₈, a process that requires the functional VIH-kinase domains. At the transcriptional level, both *TaVIH1* and *TaVIH2* are expressed in different wheat tissues, including developing grains, but show selective response to abiotic stresses during drought-mimic experiments. Ectopic overexpression of TaVIH2-3B in Arabidopsis confers tolerance to drought stress and rescues the sensitivity of *Atvih2* mutants. RNAseq analysis of TaVIH2-3B-expressing transgenic lines of Arabidopsis shows genome-wide reprogramming with remarkable effects on genes involved in cell-wall biosynthesis, which is supported by the observation of enhanced accumulation of polysaccharides (arabinogalactan, cellulose, and arabinoxylan) in the transgenic plants.

Conclusions: Overall, this work identifies a novel function of VIH proteins, implicating them in modulation of the expression of cell-wall homeostasis genes, and tolerance to water-deficit stress. This work suggests that plant VIH enzymes may be linked to drought tolerance and opens up the possibility of future research into using plant VIH-derived products to generate drought-resistant plants.

Keywords: Inositol pyrophosphate kinase, Wheat, Drought stress, Phytic acid, Transcriptome, Cell wall

* Correspondence: pandeyak@nabi.res.in; pandeyak1974@gmail.com

† Anuj Shukla and Mandeep Kaur contributed equally to this work.

¹National Agri-Food Biotechnology Institute (Department of Biotechnology),

Sector 81, Knowledge City, S.A.S. Nagar, Mohali-140306, Punjab, India

Full list of author information is available at the end of the article



© The Author(s). 2021 **Open Access** This article is licensed under a Creative Commons Attribution 4.0 International License, which permits use, sharing, adaptation, distribution and reproduction in any medium or format, as long as you give appropriate credit to the original author(s) and the source, provide a link to the Creative Commons licence, and indicate if changes were made. The images or other third party material in this article are included in the article's Creative Commons licence, unless indicated otherwise in a credit line to the material. If material is not included in the article's Creative Commons licence and your intended use is not permitted by statutory regulation or exceeds the permitted use, you will need to obtain permission directly from the copyright holder. To view a copy of this licence, visit <http://creativecommons.org/licenses/by/4.0/>. The Creative Commons Public Domain Dedication waiver (<http://creativecommons.org/publicdomain/zero/1.0/>) applies to the data made available in this article, unless otherwise stated in a credit line to the data.

Background

Inositol phosphates (InsPs) are a well-known family of eukaryotic water-soluble signalling molecules that are conserved mainly in their function [1, 2]. This family is characterized by the presence of phosphate either at the single or all the 6-carbon inositol ring backbone. The full phosphorylated InsPs (InsP₆; *myo*-inositol-hexakisphosphate, phytic acid) species can be again phosphorylated to generate high-energy Inositol pyrophosphates (PP-InsPs) [3–5]. PP-InsPs are essential members of the inositol polyphosphate family, with an array of pyrophosphate chains present at specific positions [6, 7]. The two major members of InsPs, i.e., InsP₇ and InsP₈, are present in very low abundance in cells and are synthesized by two classes of enzymes. The first class of enzyme, inositol hexakisphosphate kinases (IP6Ks), phosphorylates one of the precursors InsP₆ to form PP-InsP₅ [3, 8]. The second class of enzyme, diphosphoinositol pentakisphosphate kinases (PP-IP5Ks), phosphorylates InsP₇ to form InsP₈ /1,5PP-IP₄ [5, 9, 10].

During the past two decades, three isoforms of IP6Ks (IP6K1, IP6K2, and IP6K3) and two PP-IP5K (PP-IP5K1 and PP-IP5K2) were identified in humans and mouse [11, 12]. In yeast, a single IP6K (also referred to as Kcs1) and a PP-IP5K (also known as Vip1) are involved in the synthesis of the respective forms of InsP₇ and InsP₈ [5, 10]. These high-energy pyrophosphates participate in cellular activities such as DNA recombination, vacuolar morphology, cell-wall integrity, gene expression, pseudohyphal growth, and phosphate homeostasis as demonstrated in yeast, mice, and humans [13–19].

Earlier, the presence of high anionic forms of InsP₆ was predicted in plant species such as barley and potato [20, 21]. However, the quest to identify the plant genes encoding for these inositol pyrophosphate kinases remained elusive till the identification of two plant VIP genes from *Arabidopsis* and are present in all available plant genomes [5, 17]. In plants, VIP-homolog, also referred to as VIH proteins, contains bifunctional domains including “rimK” or ATP-grasp superfamily domain at the N-terminal and histidine acid-phosphatase domain at a C-terminus as in yeast [5, 22–24]. Furthermore, these VIH proteins displayed PP-IP5K-like activity involving in plant defense response mediated through jasmonate levels [22].

Recent evidence about genetic interaction studies implies that deletion of the VIH1 and VIH2 in *Arabidopsis thaliana* affects plant growth and is an integral part of the phosphate (Pi) response pathway [23]. The enzymatic properties of *Arabidopsis* VIH1 and VIH2 suggest that both could utilize PP-InsP₅ as a substrate, akin to the human PP-IP5K2 activity [9, 23]. Additionally, these VIH proteins were functionally active and could rescue invasive growth through hyphae formation in yeast

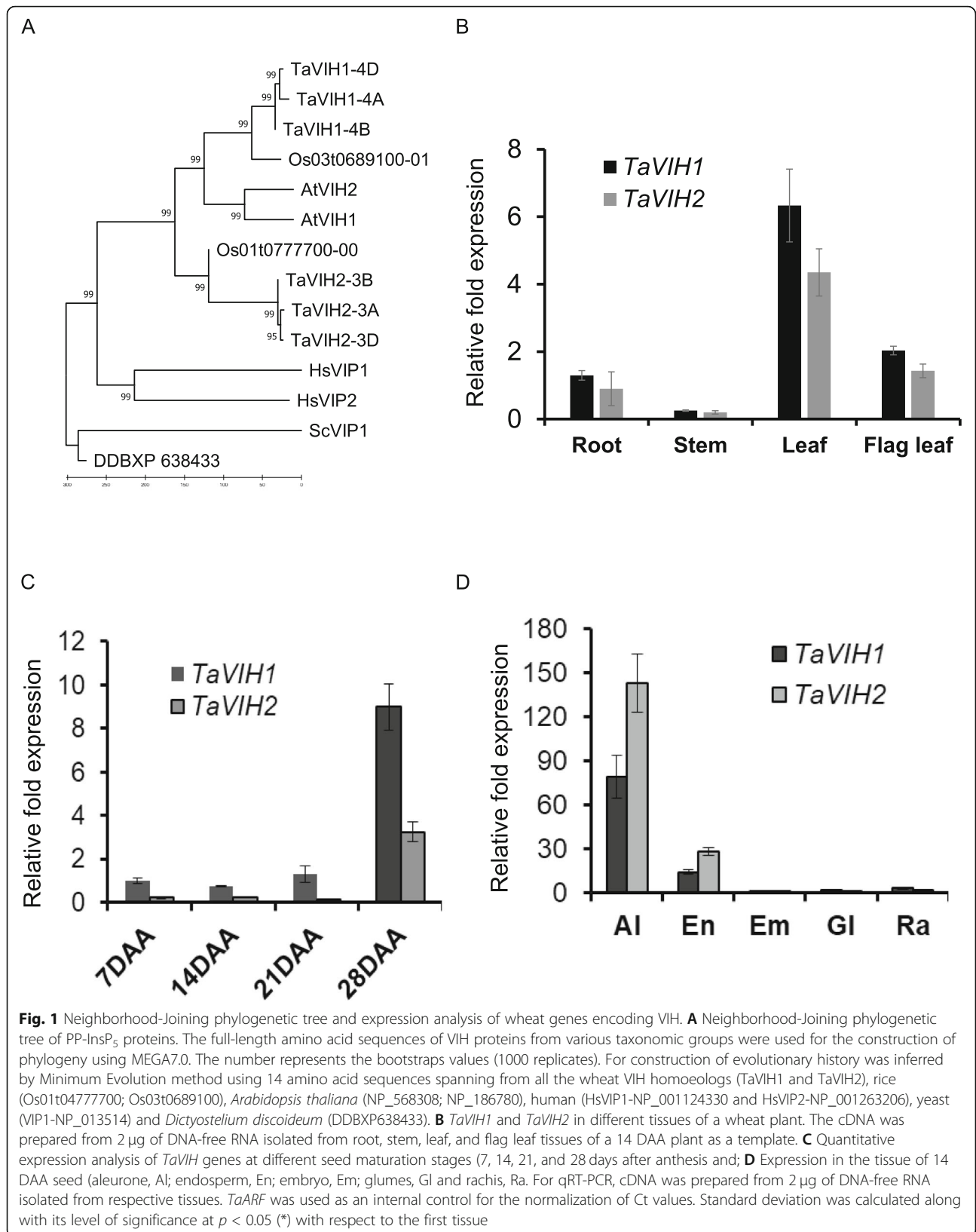
vip1Δ mutants [25]. The new line of evidence also suggested that the generated InsP₈ could bind the eukaryotic SPX domain and thereby regulate the activity of the phosphate starvation response1 (PHR1), a central regulator of phosphate (Pi) starvation [17, 23]. The conserved role of VIH kinases in synthesizing PP-InsP_x are essential for their role in Pi homeostasis as demonstrated in yeast, humans, and plants [17, 24, 26]. Thus, the role of plant VIH and PP-InsPs need further investigation to explore their additional molecular functions.

In summary, to date, the studies could reveal the function of plant VIH only in pathogen defense and Pi-limiting conditions. Still, no other role has been investigated or reported for these genes in *Arabidopsis* or other crop plants. Hexaploid wheat, an important crop around the globe and its productivity, can be affected when exposed to abiotic stress [27]. In the current study, we have identified two functionally active VIH genes from hexaploid wheat (*Triticum aestivum* L.), capable of utilizing InsP₇ as a substrate to generate InsP₈. We have performed expression studies, physiological investigations accompanied by forward and reversed genetic approaches. Our work shows that wheat VIH2 could impart tolerance to drought in transgenic *Arabidopsis*. Further, we observed that the drought tolerance was dependent upon distinct transcriptomic re-arrangements in addition to alterations in the composition of plant cell wall. Together, our study provides novel insight into the possible function of plant VIH towards stress tolerance.

Results

Phylogeny and spatio-temporal characterization of VIH genes in wheat tissue

Our efforts to identify potential wheat VIH-like sequences revealed two genes with three homoeologues each referred to as TaVIH1 and TaVIH2 showing, 98.8% sequence identity with each other. *TaVIH1* and *TaVIH2* were mapped to chromosomes 3 and 4, respectively. Both the wheat VIH genes were present on all the three genome-homoeologs (A, B, and D). The Kyte-Doolittle hydrophathy plots indicated that wheat VIH proteins were devoid of any transmembrane regions (Additional file 1: Fig. S1A and Additional file 2: Table. S1). Phylogenetic analysis clustered plant VIH homologs together with TaVIH proteins close to *Oryza sativa* (~90%) in the monocot-specific clade (Fig. 1A). TaVIH2 is closer to AtVIH1 and AtVIH2 in the phylogenetic tree with an identity of 72% and 33% with ScVIP1, respectively. TaVIH1 reveal a high identity of 78% with *Arabidopsis* (AtVIH) proteins and 35% with yeast (ScVIP1) proteins but present in different clad of the tree (Fig. 1A). Among themselves, wheat VIH1 (TaVIH-1) and VIH2 (TaVIH-2) show 70% sequence identity at the protein level (Additional file 3: Fig. S2). Amino acid sequence alignment of



wheat VIH protein sequences suggested the presence of conserved dual-domain architecture with two distinct domains consisting of N-terminal rimK/ATP GRASP fold and a C-terminal histidine acid-phosphatase (HAP) of PP-IP5K/VIP1 family (Additional file 1: Fig. S1B).

Transcript accumulation of *TaVIH* genes showed similar expression profiles for both genes, with the highest expression in leaf tissues followed by flag leaf and root and slightest expression in the stem of wheat (Fig. 1B). These findings suggest that both VIH genes are preferentially expressed in leaf (Fig. 1B). The highest expression of both VIH genes was observed at late stages of grain filling with high transcript accumulation at 28 DAA stage (Fig. 1C). Similar levels of transcript accumulation were found in the remaining grain tissues, *viz.* embryo, glumes, and rachis, suggesting a ubiquitous expression in these tissues (Fig. 1D). The expression profile in different grain tissues also revealed higher expression of *TaVIH2* genes in the aleurone layer and endosperm tissue which is ~2-fold higher than *TaVIH1* (Fig. 1D). Thus, our analysis shows differential expression patterns of VIH in different wheat tissue.

Wheat inositol pyrophosphate kinase demonstrates PP-IP₅K activity

Yeast complementation assay of wheat *VIH* genes was performed using yeast growth assay on SD-Ura plates supplemented with 0, 2.5, and 5 mM 6-azauracil. The expression of both *TaVIH1-4D* and *TaVIH2-3B* in yeast was confirmed by western blotting (Additional file 4: Fig. S3A). The wild type strain BY4741 showed an unrestricted growth phenotype, whereas *vip1Δ* transformed with empty pYES2 vector showed growth sensitivity at 2.5 and 5 mM concentrations of 6-azauracil [22] (Additional file 4: Fig. S3A). To our surprise, the mutant strain transformed with pYES2-*TaVIH1-4D* could not revive growth defect on selection plates, whereas the pYES2-*TaVIH2-3B* could rescue the growth phenotype of the *vip1Δ* strain. Previous studies show that under stress conditions, unlike wild type yeast, *vip1Δ* mutant does not form pseudo-hyphae [25]. The complemented *vip1Δ* strain with pYES2-*TaVIH2-3B* could also rescue this phenotype during stress by showing hyphae formation (Additional file 4: Fig. S3B) Overall, our data suggest that *TaVIH2* derived from the B genome can complement the growth defects of the *vip1Δ* strain.

In vitro kinase assay was performed using the pure protein of VIH-kinase domain (KD) (Additional file 5: Fig. S4). Firstly, we generated InsP₇ substrate using mouse IP6K1 enzyme using InsP₆. The synthesized InsP₇ was confirmed by TBE-PAGE gel (Additional file 6: Fig. S5A), and the gel eluted product was also subjected to MALDI-ToF (Additional file 6: Fig. S5B). The relative luminescence units (RLU) were recorded for *TaVIH1-KD*

and *TaVIH2-KD* using mIP6K1 generated InsP₇ as a substrate (Fig. 2A). The RLU value represents the ADP formed during the kinase reaction. Our assays show a significant increase in the RLU for both the *TaVIH* proteins in the presence of InsP₇ substrate. Among them, the wheat VIH2 showed a high fold luminescence response compared to the VIH1 protein (Fig. 2A). This kinase activity was diminished in VIH post-heat-denaturation (D-VIH), and the activity was not significantly different when compared to either enzyme-control (Ec) or substrate control (InsP₇) reactions. This conversion of ATP to ADP can be used as an indirect measurement biosynthesis of InsP₈.

The InsP₈ product generated by the above reactions was confirmed by resolving the reaction products by TBE-PAGE analysis [28]. To visualize the products on a gel, we used a higher concentration of InsP₇ substrate. As a control, we used ScVIP1-KD generated InsP₈ using InsP₇ as a substrate (Fig. 2B; lane5). The *TaVIH* proteins were incubated with InsP₇ as a substrate for two-time points (1 and 2 h), and the products were resolved by PAGE. Our experiments suggest that InsP₈ was synthesized only by *TaVIH2-KD* when InsP₇ was provided as a substrate (Fig. 2B). During this period of incubation, no detectable levels of the product were seen for the *TaVIH1-KD* reactions. In contrast, upon a longer incubation with substrates (~9 h), we observed that InsP₈ was generated by both VIH1 and VIH2 proteins (Additional file 6 : Fig. S5C), suggesting that *TaVIH1* may have a lower enzyme activity compared with *TaVIH2*. To further confirm the nature of generated phosphorylated inositol molecules, MALDI-ToF-MS was performed. The analysis of the InsP₈ band (generated by *TaVIH2-KD*) was done in the m/z range of 500 to 1000, which reveals a significant peak of 820.47 m/z (Additional file 6: Fig. S5D). The minor peak represents the theoretical mass of InsP₈ and the prominent peak corresponding to the InsP₈-acetonitrile adduct. These enzymatic and analytical experiments confirm that *TaVIH2* protein is functionally active and capable of using InsP₇ as a substrate under in vitro conditions and may possess PP-IP₅K like activity.

Expression of 35S: *TaVIH2-3B* transgenic *Arabidopsis* display robust growth

The biological functions of *TaVIH2* were analyzed by overexpressing the cDNA of *TaVIH2-3B* in Columbia (Col-0) *Arabidopsis thaliana*. In total, seven transgenic lines were pre-selected based on *TaVIH2* expression that was analyzed by western analysis (Fig. 3A). Further, four transgenic lines (#Line2-3, #Line 4-2, #Line 5-2, and #Line 6-1) were selected for characterization. We observed that at the vegetative stage, *TaVIH2-3B* transgenic *Arabidopsis* showed robust growth. Plants (14-

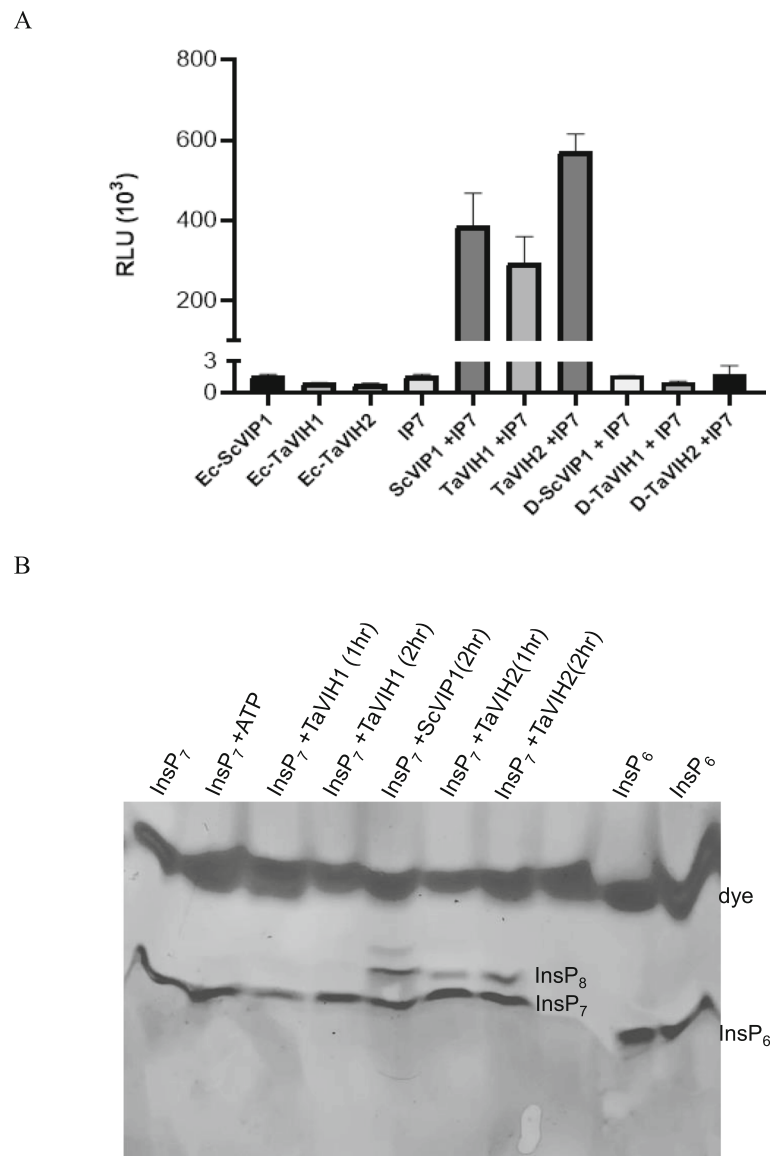


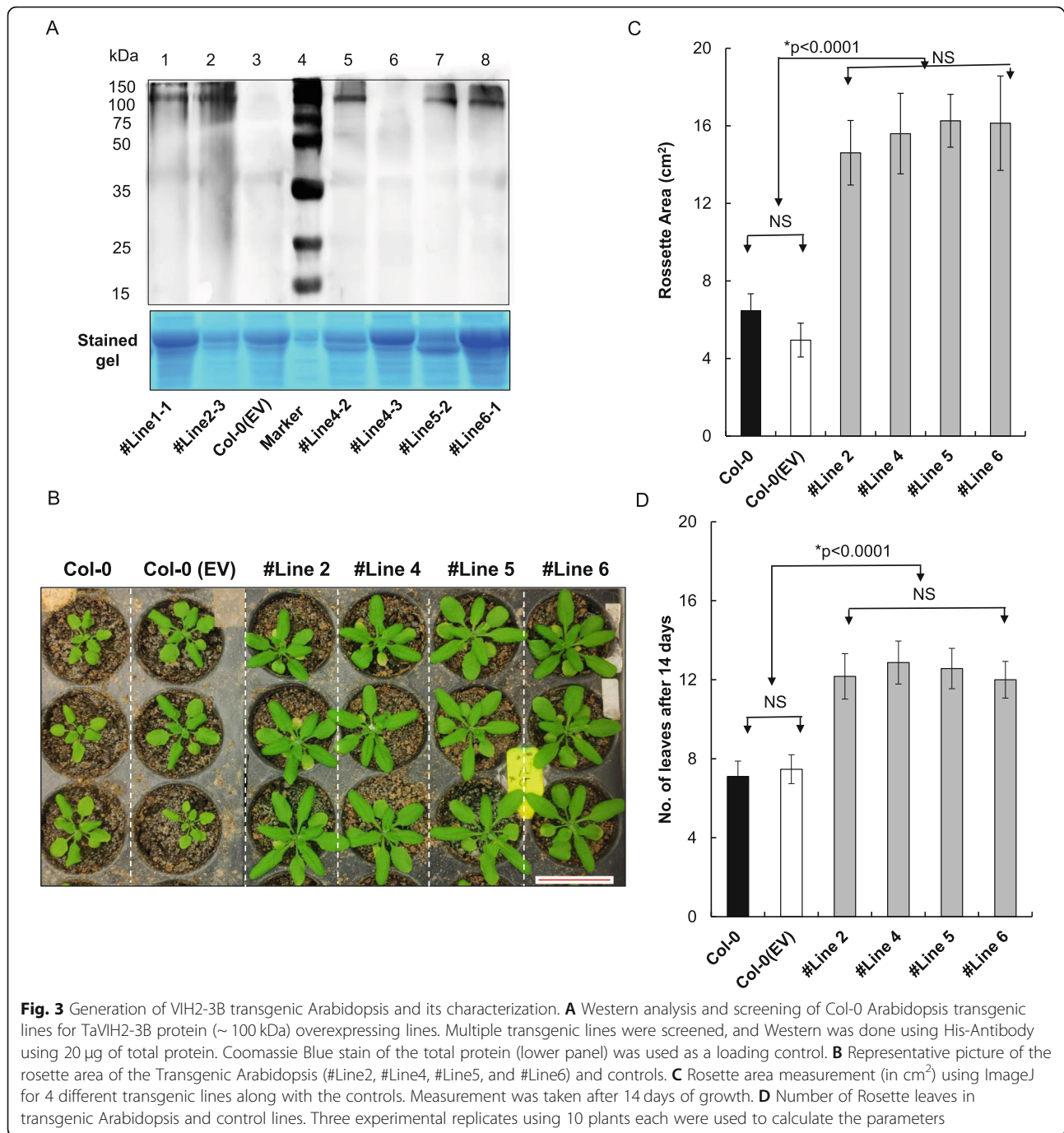
Fig. 2 Enzymatic activity and analysis of the PP-InsP on PAGE. **A** The relative luminescence units for all reactions performed were recorded using Spectramax optical reader. The kinase reactions were performed using 50 ng of TaVIH1-KD and TaVIH2-KD purified proteins for 30 min, followed by steps mentioned in the ADP-GLO kit. **B** Visualization of PP-InsP products on the PAGE gel (33%). The in vitro kinase reactions were performed using 30 ng of ScVIP1-KD, TaVIH1-KD, and TaVIH2-KD purified proteins for 1 and 2 h at 28 C. The reactions were then resolved on the gels (TBE-PAGE). The photo was taken after staining by Toluidine Blue

day-old seedlings) showed enhanced rosette area cover and increased number of leaves as compared to the controls (Col-0 and Col-0(Ev)-empty vector) (Fig. 3B–D). These transgenic *Arabidopsis* also displayed enhanced branching with an overall increase in the length of the main shoot axis and leaf size as compared to the controls (Fig. 4A, B). Primary and secondary shoot numbers were also enhanced in the transgenic *Arabidopsis* (Fig. 4D). In general, no significant differences during the flowering stage was observed, yet the increased number of (20–24) secondary shoots were evident when

compared with control plants (12–15 shoots) (Fig. 4D, E). These results suggest that the expression of TaVIH2-3B in *Arabidopsis* impacts the overall growth of the plant.

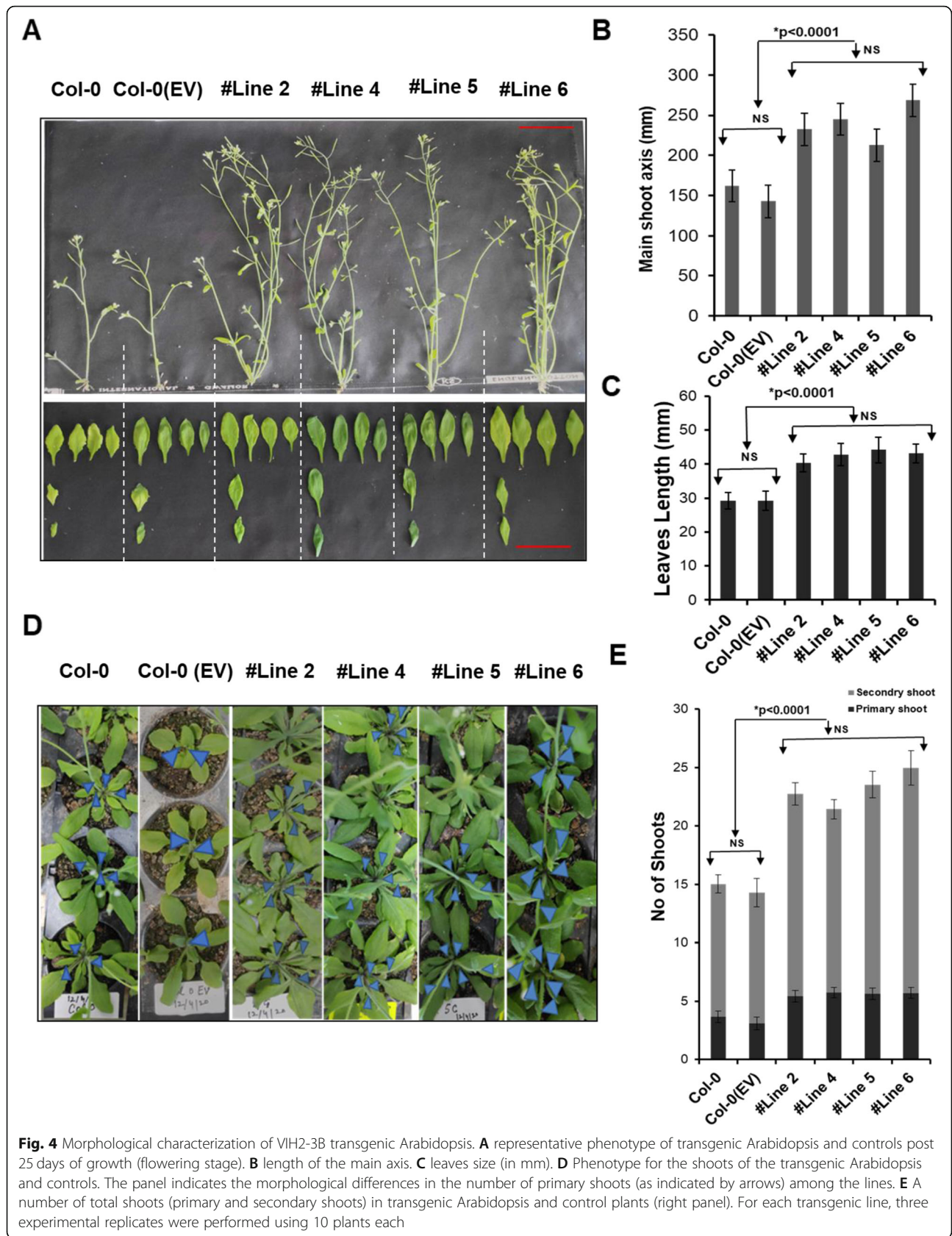
Wheat VIH2-3B respond to drought-mimic stress

To investigate the promoter activities of *TaVIH1* and *TaVIH2*, 5' flanking regions (1 kb) of these genes were cloned, and the comparative analysis revealed the presence of hormones and abiotic stress-responsive cis-elements (Additional file 7: Fig. S6A). The presence of



these elements suggested that wheat *VIH* could be regulated by stress. Notably, we observed the presence of the cis-elements that could respond to drought/dehydration, P1BS (PHR1 binding site), and GA-responsive domains. (Additional file 7 : Fig. S6A). This motivated us to perform preliminary screening experiments using *TaVIH*-promoters fused to β -glucuronidase (GUS)-reporter gene (*pVIH1/2:GUS*) in *Arabidopsis* (Col-0). A significant increase in GUS reporter activity of *pVIH2:GUS* lines indicated the ability of this promoter to sense the given

stress and drive GUS reporter expression. Interestingly, the *TaVIH2* promoter responded strongly to dehydration/drought stress and Pi starvation (Additional file 7 : Fig. S6B). Subsequently, the GUS was expressed strongly during the presence of 30% PEG (Fig. 5A). This suggests the potential role of *TaVIH2* during the drought response. A weak expression of the *TaVIH2* promoter was observed in the presence of ABA and GA₃ (Additional file 7 : Fig. S6B). Control (EV) seedlings showed no visible GUS staining. Based on our reporter assays, we



speculate that *TaVIH2* could have an essential role during a drought stress response, which was investigated further.

We tested the gene response to drought-like conditions on plant physiology. Here, seedlings were exposed to drought-like conditions using mannitol (125 mM) and glycerol (10%) [29]. No significant difference in the root growth pattern on the ½ MS plates was observed in all the *Arabidopsis* seedlings (Fig. 5B). Inhibition of the root growth was observed for the control *Arabidopsis* suggesting their sensitivity to the presence of both the mannitol and glycerol (Fig. 5B). In contrast, *TaVIH2-3B* overexpression in *Arabidopsis* was able to escape the detrimental root growth (Fig. 5C). Finally, to check the sensitivity of *Arabidopsis vih2-3/vih2-4* and its rescue by wheat *VIH2*, we screened the complemented mutant lines with *TaVIH2-3B* and evaluated it during drought-mimic conditions (Fig. 6A). Interestingly, both *vih2-3* and *vih2-4* showed high sensitivity towards drought-mimicking conditions and this sensitivity was restored to similar to Col0-(EV) when complemented with *TaVIH2-3B* (Fig. 6B, C). These results corroborate the intriguing aspects of *TaVIH2* physiological function during drought stress.

Wheat *VIH2-3B* imparts resistance to water-deficit stress

Studying the relative water loss helped us investigate the direct involvement of *TaVIH2-3B* in conferring the drought tolerance in the detached leaves. The rate of water loss was very significant in the control plants compared to the transgenic plants (Fig. 7A). This loss was less in the transgenic *Arabidopsis* (40–46%) when compared to control plants (16–18%) after 8 h of incubation (Fig. 7A). Next, we measured relative leaf water content (RWC%; Fig. 7B) for these plants. The RWC was high (~ 65%) in transgenic plants as compared to the control plants (~ 46%).

Further, drought stress experiments were carried out for all the plants by exposing 7-day-old plants to 14 days of water withholding (drought). These experiments were carried out for the mutant, wild type, and overexpressing plants together in the same pot for ensuring that they are inter-rooted and exposed to the same soil moisture conditions. After 14 days of drought, the relative soil moisture content was observed to be as low as 35% in the pots. This caused a dramatic withering of both control and transgenic *Arabidopsis* plants. However, when the plants were re-watered, high survival rates (~ 65%) were observed in the transgenic plants, whereas no or very low (3%) survival efficiency was observed in control. No survival was observed for the *vih2-3* mutant plants (Fig. 7C), indicating their sensitivity to drought conditions. This indicates that the transgenic *Arabidopsis* overexpressing *TaVIH2* escapes the effect of drought

and improves survival rate by imparting drought tolerance.

Transcriptomics data suggest that *VIH2-3B* stimulate genes related to drought stress

In order to understand the basis of robust phenotype and drought resistance observed in the transgenic *Arabidopsis* plants when complemented with *TaVIH2-3B*, we used the transcriptomics approach. Transcriptomics changes in 25-day-old seedlings of control and two transgenic plants (#Line4 and #Line6) were analyzed. PCA of normalized expression abundances revealed a high level of correlation among biological replicates ($n = 3$) in each transgenic line. PCA also indicates a distinct cluster for overexpressing transgenic lines and controls (Additional file 8 : Fig. S7A). Based on an analysis involving respective three biological replicates, a total of 626 and 261 genes were significantly up- and downregulated ($-1 > \text{Log FC} > 1.0$) in #Line4 while 797 and 273 genes were up- and downregulated in #Line6 transgenic *Arabidopsis* lines compared to control plants (Additional file 9 : Table S2). Overall, 605 genes were commonly differentially altered in the two transgenic lines with respect to the control plants (Col-0(Ev); Fig. 8A).

Interestingly, a high number of genes constitutively activated in the transgenic *Arabidopsis* belong to the dehydration response element-binding (DREB) protein, including Integrase-type DNA-binding superfamily proteins and glycine-rich proteins. Upon analysis of the GO terms, the highest number of genes for “stress-related” and “cell-wall-related activities” were enriched in the biological process and cellular component categories (Fig. 8B and Additional file 8 : Fig. S7B). Strikingly, multiple genes involved in cell-wall biosynthesis, modification and degradation were also upregulated in the transgenic plants (Fig. 9A). In addition to that, distinct clusters of genes involved in abscisic acid (ABA) biosynthesis were also significantly upregulated among the different lines of transgenic *Arabidopsis* (Fig. 9B). Notably, drought-marker genes encoding 9-*cis*-epoxycarotenoid dioxygenase (*AtNCED6* and *AtNCED9*) involved in ABA biosynthesis were also upregulated. Multiple DREB encoding genes and cytochrome P450 (CYPs)-related family genes (*CYP71A23*, *CYP94B3*, *CYP71B12*, *CYP96A2*, *CYP702A1*, *CYP707A3*, *CYP82C2*, *CYP76G1*, *CYP705A4*, *CYP71B10*, *CYP706A2*, *CYP81D11*) were also differentially regulated in the transgenic *Arabidopsis* (Fig. 9C, D). The expression response of these genes was also validated by using qRT-PCR analysis. Our expression data strongly supported the transcriptome observation that reflects the upregulation of multiple genes (Additional file 10 : Fig. S8). These genes validate the abundance of transcripts encoding for DREB, ABA biosynthesis, and CYP sub-family genes in transgenic lines when

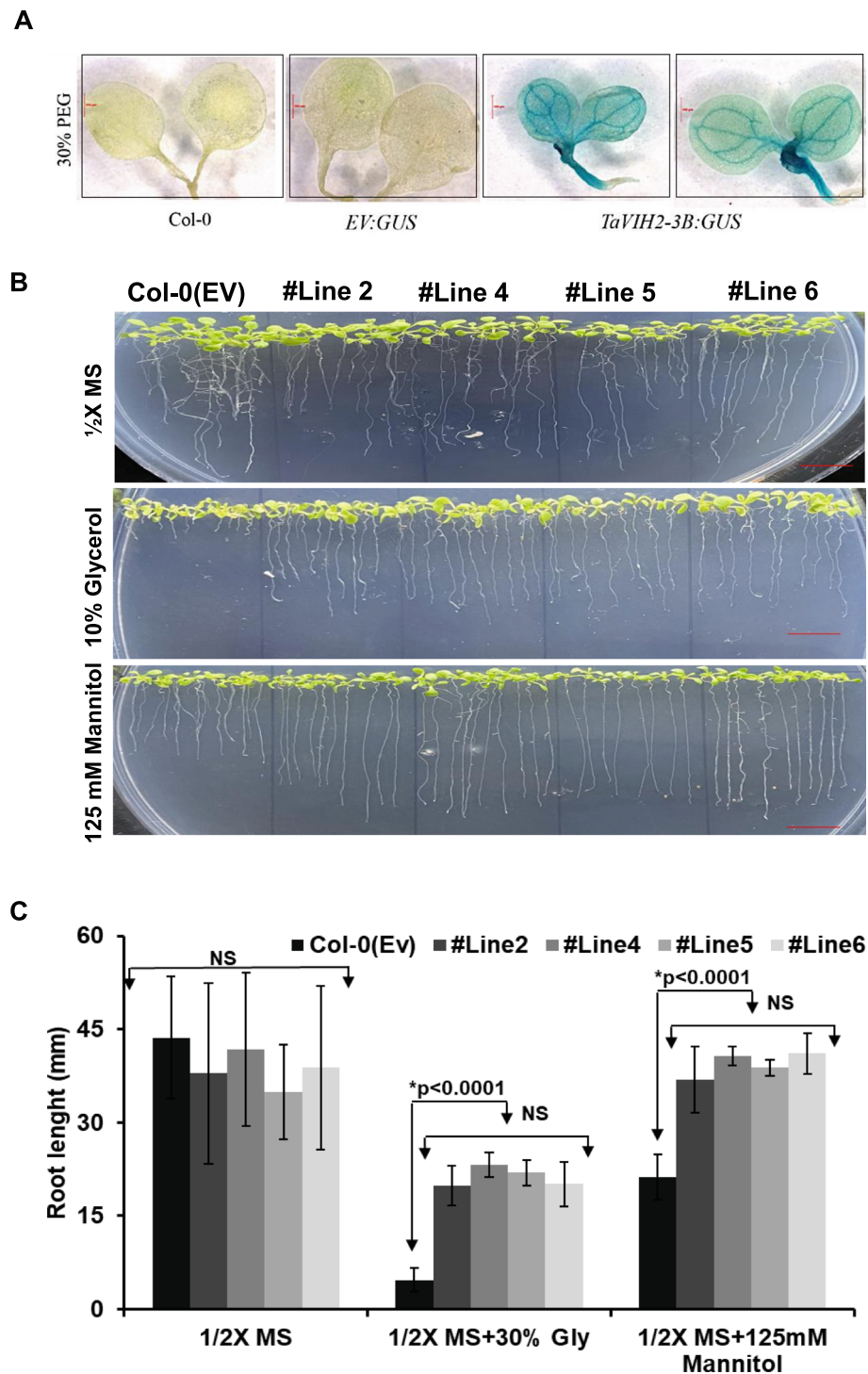


Fig. 5 Drought-mimic stress for VIH2-3B *Arabidopsis* transgenic lines. **A** Reporter assays using promTaVIH2:GUS transgenic lines subjected to drought-mimic (30% PEG). Seedlings with or without treatment (control) were stained overnight in GUS staining solution and photographed using a Leica stereomicroscope at $\times 6.3$ magnification. **B** Transgenic *Arabidopsis* and control seedlings were subjected to drought-mimic conditions with glycerol (10%) and mannitol (125 mM). Ten seedlings were used for each transgenic line for each treatment. These experiments were repeated in three experimental replicates with a similar phenotype. **C** Root length of treated seedlings (in mm) for all the lines. Twenty seedlings were used for the measurement of root length for each line

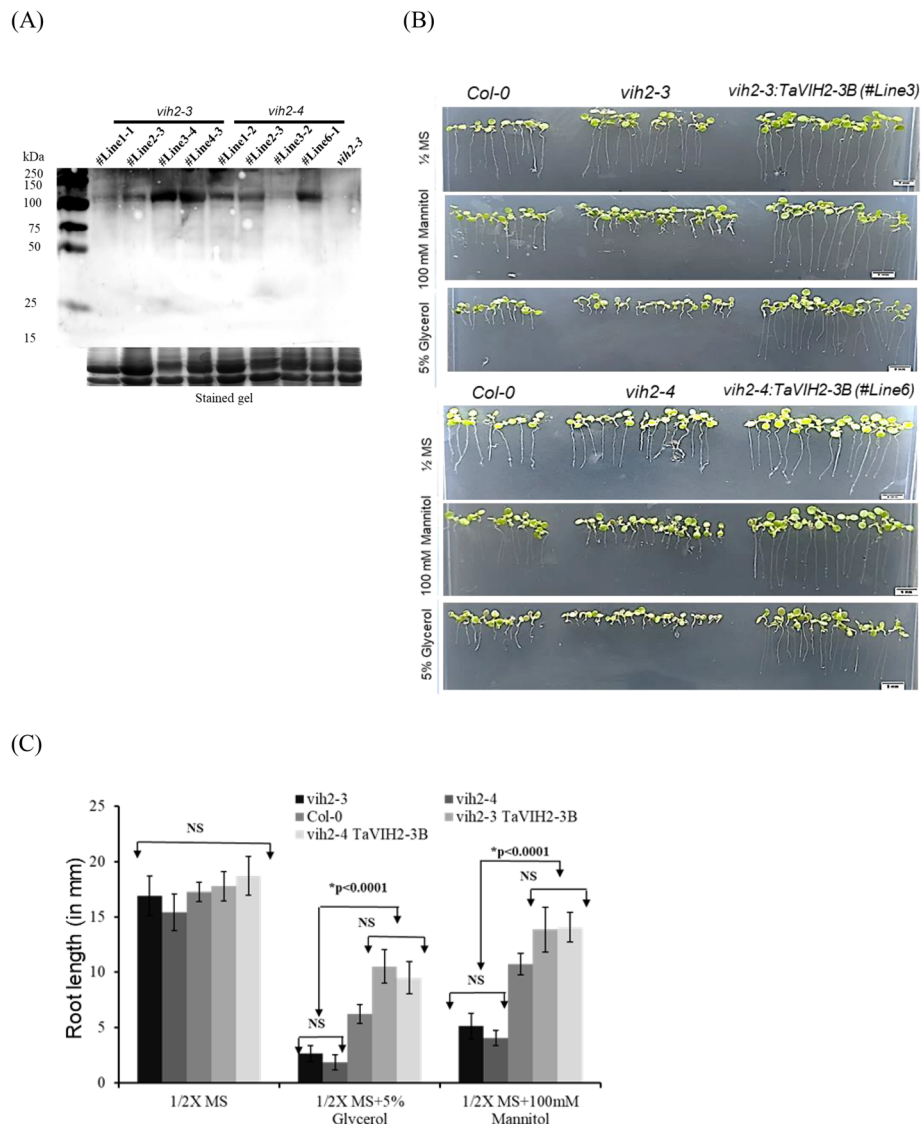


Fig. 6 Complementation of *vih2-3* line and its characterization. **A** Western analysis of *vih2* mutant lines (*vih2-3* and *vih2-4*) complemented with *TaVIH2-3B*. Multiple transgenic lines were screened and Western was done using His-Antibody using 20 µg of total protein. Coomassie Blue stain of the total protein (lower panel) was used as a loading control. **B** Transgenic *Arabidopsis*, mutant and *Col-0* seedlings were subjected to drought-mimic conditions with glycerol (5%) and Mannitol (100 mM) (for moderate mimic-drought). Eight to ten seedlings were used for each transgenic line for each treatment. **C** Root length in mm ($n = 20$). These experiments were repeated three experimental replicates with similar phenotype and ten plants each

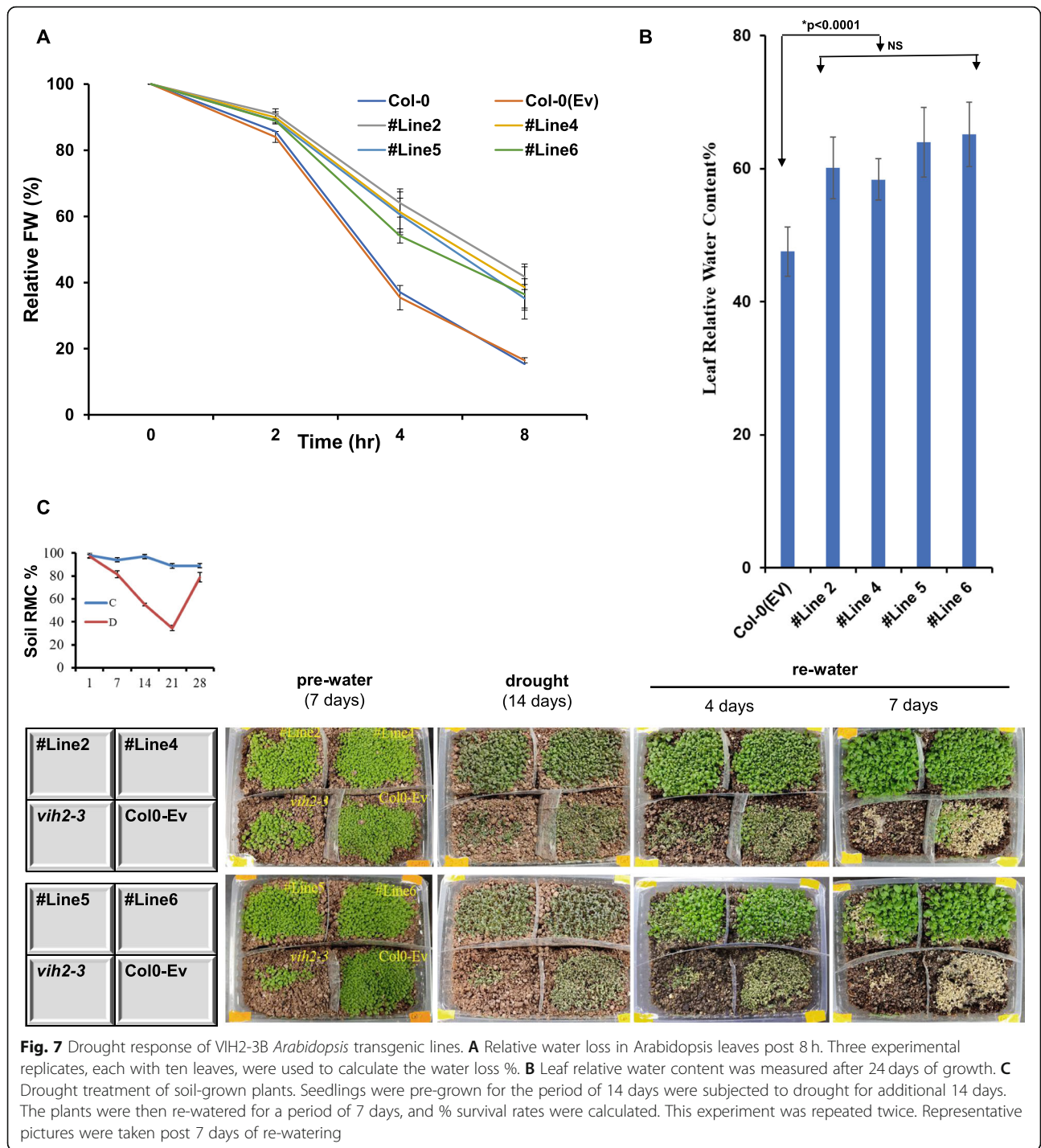
compared to wild type. Overall, we conclude that a distinct cluster of genes involved in drought and ABA stress were significantly upregulated in these transgenic plants and thus may impart tolerance to stress.

VIH2 overexpression affects ABA levels and regulates plant cell-wall composition

Multiple genes related to ABA biosynthesis were differentially expressed in *TaVIH2-3B* overexpressing *Arabidopsis*. To verify if the de novo gene expression response to ABA-associated genes could be correlated with its

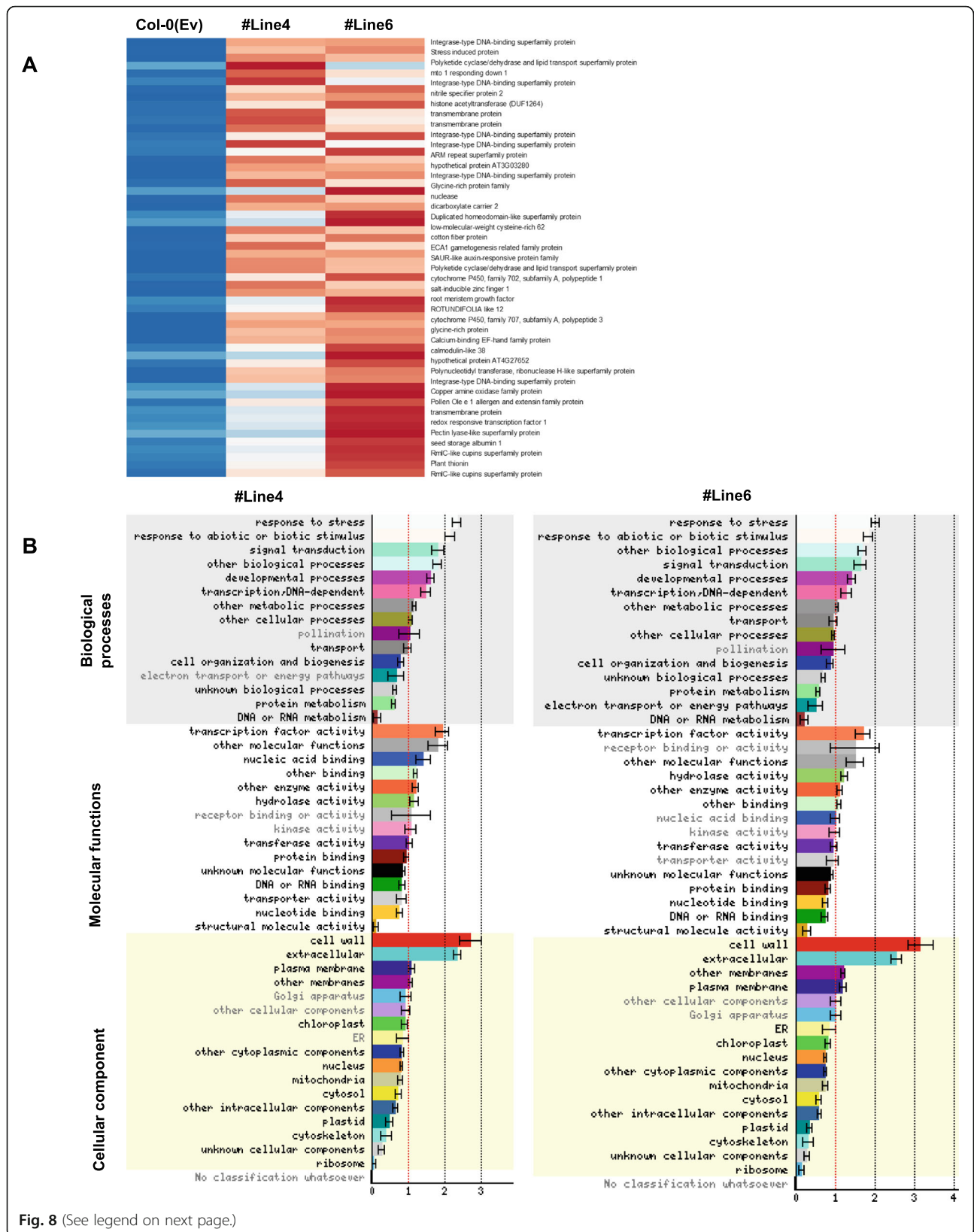
in vivo levels, ABA was quantified in their leaves. We observed that the accumulation of ABA was significantly higher (~ 3–4 fold) in transgenic *Arabidopsis* when compared to the control plants (Fig. 10A). This average increase of ABA in all the four transgenic lines was statistically significant ($p < 0.0001$, Student’s *t* test). Our data confirmed the involvement of ABA in the drought tolerance of transgenic lines.

Our results have revealed the function of *TaVIH2-3B* in drought stress. To draw the commonality between our gene expression in *TaVIH2-3B* overexpressing



Arabidopsis and drought, we analyzed previously reported RNAseq data SRA: SRP075287 (under drought stress) for overlap of de-regulated genes. In total, 295 and 309 genes were commonly regulated in #Line4 and #Line6 when compared with drought data (Fig. 10B and Additional file 11 : Table S3). Most of the listed genes that were commonly regulated belong to the category of hormone metabolism, signalling, stress response,

development and cell-wall functions (Fig. 10C). Multiple genes NCEDs, CYPs, and glycosyltransferases were highly enriched in the dataset (Additional file 11 : Table S3). These extended analyses support the notion that TaVIH2-3B could impart activation of genes pertaining to drought in transgenic plants that could impart basal drought resistance. Since cell-wall plays a significant role in imparting drought resistance, we, therefore, measured



(See figure on previous page.)

Fig. 8 RNAseq analysis of Col-0 and #Line4 and 6. **A** Expression pattern (as Z-scores) of top 56 genes commonly upregulated among the transgenic lines w.r.t. Col-0(Ev) in 25-day-old seedlings. Heatmap depicts the relative expression in Col-0(Ev) and overexpressing lines of *TaVtH2-3B* (3 biological replicates; rep1-3). **B** Heatmap representing a graphical summary of the Gene Ontology (GO) classification for DEGs in #Line4 and #Line6 w.r.t. Control plants. Increasing intensities of brown and blue colors represent the comparatively low and high expression for each gene, as depicted by the color scale. Normalized expression counts were used to plotting the expression as Z-scores using heatmap. Two functions from the gplots package in R. Significantly altered GO terms were identified using the Classification SuperViewer tool; the x-axis represents the GO terms where bold terms represent significant alteration while the y-axis represents the normed frequency which when > 1 signifies over-representation while < 1 signifies under-representation

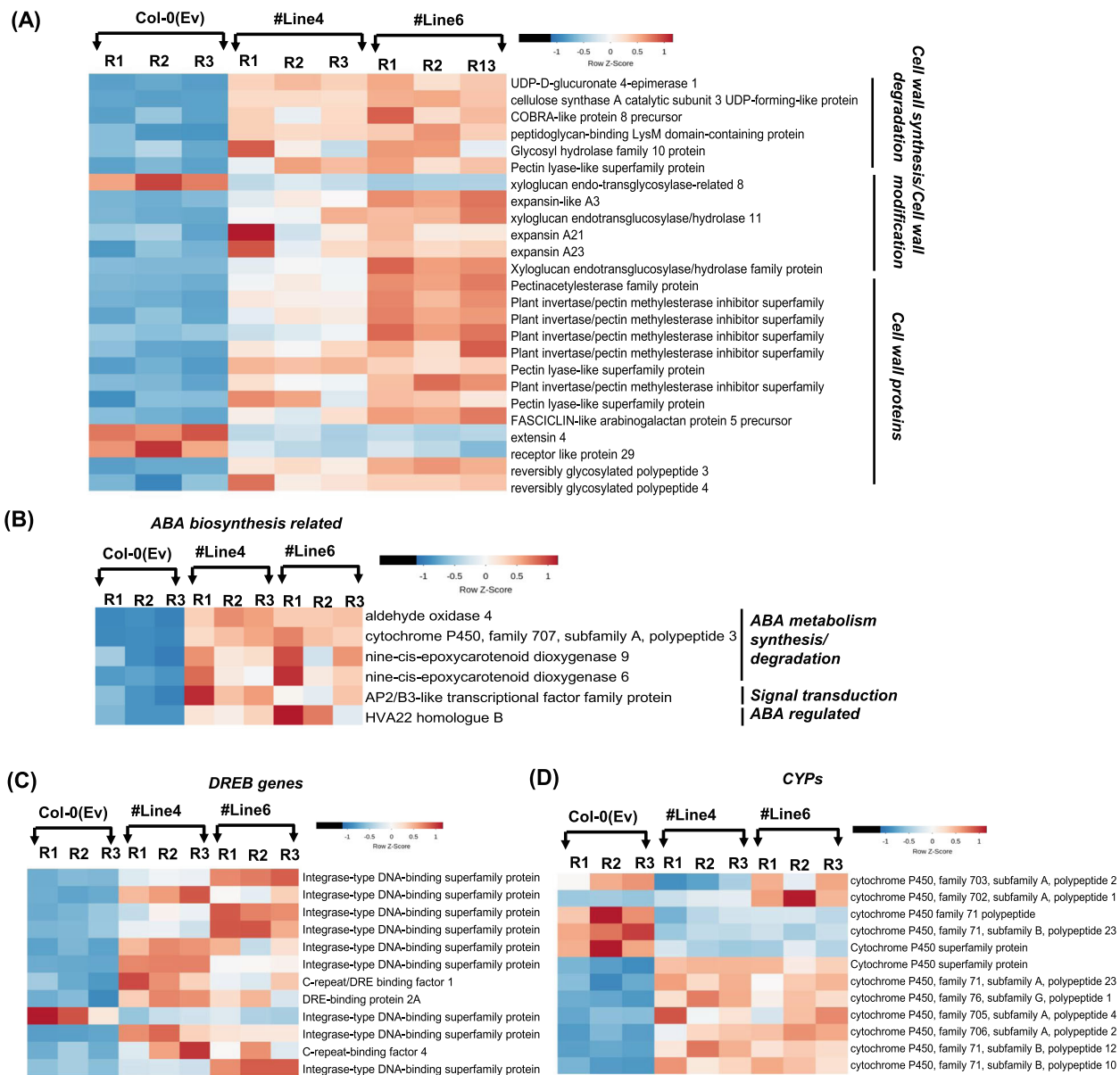
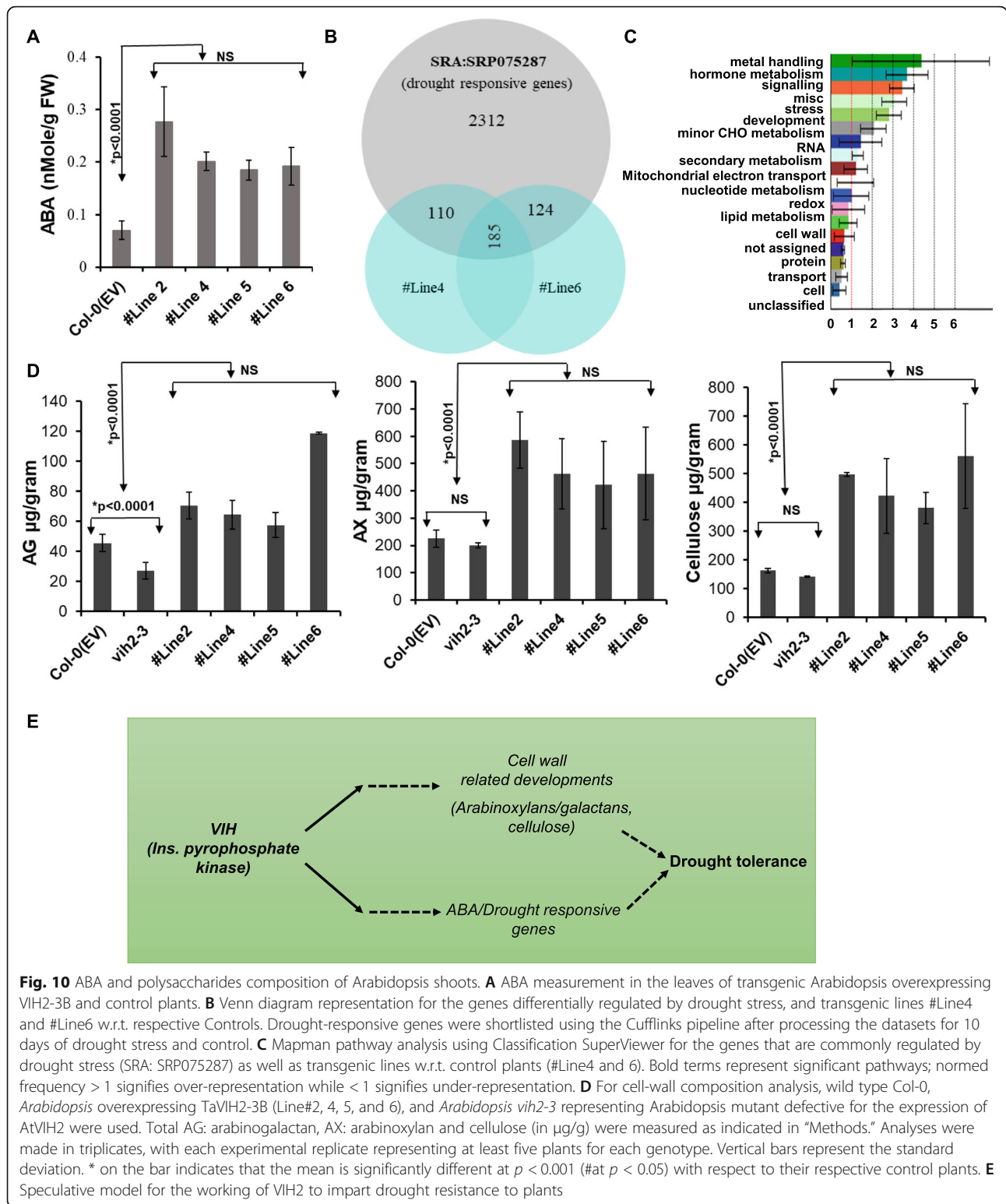


Fig. 9 Heatmap expression analysis of gene families in Col-0(Ev) overexpressing *TaVtH2-3B* Arabidopsis (#Line4 and 6). **A** Heatmaps for expression patterns (as Z-scores) for genes DE in both transgenic lines w.r.t. Col-0(Ev), encoding for the genes involved in cell-wall homeostasis. **B** ABA biosynthesis-related pathway genes. **C** DREB encoding genes. **D** cytochrome P450 (CYPs) genes. Increasing intensities of brown and blue colors represent the comparatively low and high expression for each gene, as depicted by the color scale. Normalized expression counts were used to plotting the expression as Z-scores using heatmap. Two functions from the gplots package (Warnes et al., 2005) in R. Genes encoding for respective pathways were extracted using MapMan (Thimm et al., 2004). R1, R2, and R3 represent the biological replicates for the RNAseq analysis of the individual lines



different cell-wall components of control and transgenic Arabidopsis. Using standard extraction methods resulted in comparable yields from all the tested plants, and the presence of starch was ruled out before performing

experiments. Our extraction procedures for control plants show the ratio of 1:1.2 to 1.5 for arabinose/galactose and arabinose/xylans. This validates our extraction procedures. Our analysis indicated a consistent increase

in the accumulation of cellulose (from 1.3 to 2.5-fold) in the transgenic lines that were the same among the biological replicates and multiple transgenic lines (Fig. 10D). Additionally, arabinoxylan (AX) and arabinogalactan (AG) was also increased (1.8–2.2 and 1.47–1.5-fold) in the transgenic lines as compared to the controls (Fig. 10D). To further validate the role of VIH proteins, the *Atvih2-3* mutant line was used for measuring the biochemical composition of the shoot cell wall (Fig. 10D). Our analysis showed a significant reduction of the AG, AX, and cellulose content in this mutant line when compared to transgenic lines (Fig. 10D). Our data demonstrate that overexpression of wheat VIH2-3B resulted in changes in the cell-wall composition, and these changes could be linked to the enhanced drought response in leaves.

Discussion

Recently, studies investigating inositol pyrophosphates have gained much attention due to the presence of high-energy pyrophosphate moieties speculated to regulate metabolic homeostasis in organisms [22, 25, 30–32]. This study was performed to characterize and identify the functional mechanism of VIH proteins involved in the biosynthesis of PP-InsPx. We have characterized two wheat inositol pyrophosphate kinase (TaVIH1 and TaVIH2) encoding genes and demonstrated that homoeolog wheat *VIH2-3B* in *Arabidopsis* could enhance growth and provide tolerance to drought stress. Our line of evidence shows that this tolerance to drought is a result of the ability of VIH to modulate cell-wall- and ABA-related genes resulting in the changes in the cell-wall polysaccharide composition (AG, AX, and cellulose).

Hexaploid bread wheat has one of the most complex genomes comprising of three related sub-genomes that have originated from three separate diploid ancestors, thus forming an allohexaploid genome [33, 34]. Therefore, to consider the appropriate homoeolog-transcript for further studies, the Wheat-Exp expression database was used to analyze VIH2-3B homoeolog expression in different tissues and also during the developmental time course (Additional file 12 : Fig. S9A). Plant VIHs are known to be involved in defense response via a jasmonate-dependent resistance in *Arabidopsis* [22]. Wheat VIH genes were also induced upon infection of plants with pathogens (Additional file 12 : Fig. S9B and C). Thus, the role of plant VIH genes during plant-microbe interaction was found to be conserved. TaVIH protein was an authentic kinase protein since its kinase domain could catalyze phosphorylation and harbors yeast VIP1-like activity, as demonstrated by its utilization of InsP₇ as a substrate. In the past, AtVIH proteins possess kinase activity that generates different

isoforms of InsP₇ [22, 25]. Earlier, it was suggested that *Arabidopsis* VIH2 executes Vip1/PP-IP5K but not Kcs1/IP6K-like activities in yeast [22]. This observation confirms the conserved kinase activity among the plants with high substrate affinity for InsP₇ [35]. Similarly, yeast and human enzymes also show differential InsP₆ and InsP₇ kinase activity [5, 36, 37]. We tested InsP₇ as a substrate for wheat VIH proteins where TaVIH2 shows more specificity towards InsP₇ that suggest PP-IP5K-like activity generating InsP₈ (Fig. 2B). Intriguingly, our time-dependent assays and the RLU value, which reflects the conversion of InsP₇ to InsP₈, could account for the different affinity of wheat VIH proteins (Fig. 2A, B). Interestingly, AtVIH1 and AtVIH2 show a high identity (89.8%) at the protein level, whereas specifically TaVIH1-4D and TaVIH2-3B arising from two different chromosomes show 72% identity. VIH protein alignment of *Arabidopsis* and wheat suggest the presence of the conserved residues required for protein-substrate (5-InsP₇) interactions (Additional file 3 : Fig. S2). Although the conserved-catalytic residues remain same in both the wheat VIH proteins, we could still see changes in the protein sequences in the N-terminal ATP-grasp domains. Wheat genome encodes a total of six VIH proteins that remains to be tested if they could vary in the affinity to utilize the respective substrates. These apparent differences could be intriguing that requires further biochemical investigations.

The presence of various *cis*-acting elements in the promoter region plays an essential role in the transcriptional regulation of genes in response to multiple environmental factors. Our transcriptional activity of *TaVIH2-3B* promoter and expression analysis links TaVIH2-3B with Pi starvation response (Additional file 3 : Fig. S2). This function of inositol pyrophosphate kinases in the regulation of Pi homeostasis seems to be evolutionarily conserved [31, 37]. In *Arabidopsis*, it was recently demonstrated that VIH-derived InsP₈ is required to sense the cellular Pi status and binds to the intracellular Pi sensor SPX1 to control Pi homeostasis in plants [24]. We found that in addition to Pi homeostasis, the *TaVIH2-3B* promoter also responds to drought conditions.

Earlier, the double mutants of VIH genes in *Arabidopsis* show severe growth defects, implicating their unexplored role in overall growth and development [23]. We hypothesize that the molecular and biochemical changes in transgenic *Arabidopsis* provide the overall mechanical strength to the plant cell and, in turn, tolerance to stress conditions. These observations were also supported by our transcriptome analysis of two independent TaVIH2-3B overexpressing *Arabidopsis* lines that show consistent high expression of cell wall, ABA, and DREB genes (Fig. 8 and Fig. 9B). Multiple genes were differentially

regulated by *TaVIH2-3B* overexpression, suggesting that increased protein levels of VIH2 could cause changes in gene expression patterns. Classically, VIH proteins contain evolutionarily conserved two distinct domains, including an N-terminal rimK/ATP GRASP kinase and phosphatase domain. It remains to be dissected if the change in transcriptome response in these transgenic *Arabidopsis* is due to the kinase or phosphatase domain. Earlier, multiple inositol-1,3,4 triskisphosphate 5/6-kinase (devoid of phosphatase domain) was also implicated for their role in drought tolerance [38, 39]. This may suggest that the tolerance for the drought could arise by the presence of the functional kinase domain.

Multiple studies have implicated that an enhanced level of ABA leads to drought tolerance [40–43]. The elevated levels of ABA in our transgenic plants could be accounted for the high expression of genes involved in cell-wall maintenance and biosynthesis. In yeast, the role of inositol pyrophosphate kinase was also implicated in vacuolar morphology and cell-wall integrity [14]. Plant cell-wall-related remodelling and ABA-regulated signalling is the primary response against abiotic stress, including drought [41, 42, 44]. ABA-dependent increased expression of NCEDs, CYPs, and *DREBP* have been reported earlier in plants with their role implicated in drought stress [40, 43, 45]. Our study shows a high basal expression of genes encoding for *DREBP* and CYPs (Fig. 8C). The high constitutive expression of these gene families in our transgenic *Arabidopsis* could account for their better adaptability for drought stress (Fig. 8A–C). ABA is an important phytohormone regulating plant growth, development, and stress responses [46, 47]. At the mechanistic level, ABA could target downstream genes that are able to support plant growth even under non-stress condition [48]. In our case, high ABA levels could be as a result of such homeostatic interaction with other hormones, although this needs to be confirmed in future. Additionally, the high expression of the subset of NCEDs and *DREB* genes could also be accounted for ABA-regulated signalling in transgenic *Arabidopsis*. Similarly, overexpression of NCED could result in high accumulation of ABA [49, 50]. Earlier, changes in cellular levels of InsP_7 and InsP_8 have been attributed to guard cell signalling, ABA sensitivity, and resistance to drought in maize *mnp5* mutants [31, 51]. This suggests a molecular link between *TaVIH2*, ABA levels, and drought resistance. Resolving the *in vivo* levels of InsP_x is technically challenging for non-specialized labs. Our current study is limited due to the lack of *in vivo* measurements of InsP_8 in these transgenic lines. *In vivo* profiling of InsP_x by enrichment with TiO_2 is a powerful tool that has been employed with plant tissue [23, 24, 52]. We are currently optimizing this method to detect the InsP_x generated in our transgenic lines. However,

TaVIH2-3B showed the highest homology to *AtVIH2* (70.6%) and both show PP-IP5K like activity. Therefore, we speculate that these transgenic plants may possess high levels of InsP_8 .

Atvih2-3 mutant lines lacking mRNA expression also show alteration in the cell-wall composition despite its typical growth as wild type Col-0 (Fig. 9D). Interestingly, *vih1* and *vih2* double mutants display severe growth defect that was rescued by the gene complementation [23]. In our study, we complemented the *vih2-3* *Arabidopsis* mutant with the *TaVIH2-3B* that resulted in restoring Col-0(Ev) like phenotype. This suggests that wheat *VIH2-3B* could functionally complement *Arabidopsis vih2* mutants, and it is possible that the *in vivo* level of InsP_8 is restored in these lines since both bear PPIP5K activity.

Our overexpression data showing enhanced branching and robust growth collectively reinforce the notion that VIH are also involved in providing support for plant growth. The *vih2* mutant in *Arabidopsis* is more susceptible to infestation by caterpillar (*Pieris rapae*) and thrips [22]. The resistance against herbivore pathogens such as *P. rapae* could be gained by modulating the genes associated with cell-wall modification [53]. *Arabidopsis vih2* lines showed compositional changes in the cell-wall-extracted polysaccharides, especially at the AG level. The decreased resistance in *vih2* mutants against herbivores could be accounted for the defect in the signalling pathway via COI1-dependent gene regulation and changes in the structural composition of the cell wall. Taken together, we propose a working model, where wheat VIH participate in the drought resistance in plants by modulating the changes in cell-wall gene expression, enhanced ABA levels, and change in biochemical composition to provide more mechanical strength (Fig. 10E). In future, it will be interesting to quantitate the level of higher inositol pyrophosphates in these plants.

Conclusions

Herein, we explored additional roles offered by plant VIH proteins. We employed genetic and biochemical tools to characterize the wheat homoeolog *VIH2-3B* as an active PP-IP5K. Our lines of evidence suggest that the expression of VIH genes is perturbed during drought conditions and could modulate the expression of genes involved in cell-wall maintenance so as to relay resistance to both mimic-drought and drought conditions. Interestingly, the wheat *VIH2* was able to complement the *vih2-3/2-4* which were also sensitive to mimic-drought-like condition. In summary, our work provides a glimpse into the emerging new role of plant VIH proteins in cell-wall scaffolding functions to provide resistance against drought stress. Future studies will be required to dissect the casual effect of drought response

that could be mediated at the protein level by the VIH2 or levels of InsPx species in these transgenic lines.

Methods

Plant materials and growth conditions

The experiments in this study were conducted using *Arabidopsis thaliana* variety Col-0 ecotype and Bread wheat (*Triticum aestivum* L.) variety “C-306” (Mishra et al., 20201). For the collection of the tissue materials, the spikes tagged on the first day after anthesis (DAA) post which samples were collected at 7, 14, 21, and 28 DAA stages and various tissues, including root, stem, leaf, and flag leaf of 14 DAA stage. For seed tissue collection, 14 DAA seed was used to separate different tissues, including aleurone, endosperm, embryo, glumes, and rachis as mentioned previously [54].

Identification and cloning of two wheat VIH genes

Two *Arabidopsis* (AT5G15070.2 and AT3G01310.2) and the previously reported yeast VIP1 sequences were used to perform Blastx analysis against the IWGSC (www.wheatgenome.org/). The identified sequences were analyzed for the presence of the typical dual-domain structure. Furthermore, the Pfam domain identifiers of the signature ATP-grasp kinase (PF08443) and histidine acid phosphatase (PF00328) domains were used to identify VIH proteins in the Ensembl database using the BioMart application. The corresponding predicted homoeologous transcripts were found and compared to the other VIH sequences. DNA STAR Lasergene 11 Core Suite was used to perform the multiple sequence alignment and calculate the sequence similarity. Gene-specific primers capable of amplifying the transcript from the specific genome was designed after performing 5' and 3'-RACE to ascertain the completed open reading frame (ORF). Subsequently, full-length primers were designed to amplify the *VIH* genes. The generated full-length sequence information was further used for qRT-PCR-related studies.

Hydropathy plot and IDR prediction

The hydropathy profile for proteins was calculated according to Kyte and Doolittle, 1982. The positive values indicate hydrophobic domains, and negative values represent hydrophilic regions of the amino acid residues. To identify the % similarity with IDR boundaries, MFDp2 (<http://biomine.cs.vcu.edu/servers/MFDp2>) was used to predict the disorder content in the input sequence [55].

Isolation of total RNA, cDNA synthesis, and quantitative real-time PCR analysis

Total RNA from various tissues was extracted by a manual method using TRIzol® Reagent (Invitrogen™). The

integrity and concentration of RNA were measured, and contamination of genomic DNA was removed by subjecting the RNA samples to DNase treatment using TURBO™ DNase (Ambion, Life Technologies). Two micrograms of total RNA was used for cDNA preparation using The Invitrogen SuperScript III First-Strand Synthesis System SuperMix (Thermo Fisher Scientific) as per the manufacturer's guidelines. qRT-PCR was performed using the QuantiTect SYBR Green RT-PCR Kit (Qiagen, Germany). The gene-specific primers capable of amplifying 150–250-bp region from all the three homoeologous of two *TaVIH* genes were carefully designed using Oligocalc software. Four technical replicates for each set of primers and a minimum of two to three experimental replicates were used to validate the experiment. Gene-specific primer (with similar primer efficiencies) used in the study are listed in Additional file 13 : Table S4. ADP-ribosylation factor gene (*TaARF*) was used as an internal control in all the expression studies. The Ct values obtained after the run were normalized against the internal control, and relative expression was quantified using the $2^{-\Delta\Delta CT}$ method [56].

For in silico expression for *TaVIH* genes, the RefSeq IDs were used to extract expression values as TPMs from the expVIP database. For different tissues and stages, the expression values were used to build a heatmap. In the case of abiotic and biotic stress conditions, the expression values from the control and stressed conditions were used to get fold change values, which were then used to plot heatmaps using MeV software.

Construct preparation for expression vector and yeast functional complementation

For complementation assays, pYES2, a galactose-inducible yeast expression vector, was used. The functional complementation of yeast by TaVIH proteins (with C-myc tag) was studied using 6-azauracil-based assay. The wild type BY4741 (MATa; his3D1; leu2D0; met15D0; ura3D0) and *vip1Δ* (BY4741; MATa; ura3Δ0; leu2Δ0; his3Δ1; met15Δ0; YLR410w::kanMX4) yeast strains were used for the growth assays. The CDS corresponding to the catalytic domain of *ScVIP1* (1-535 amino acids) cloned into pYES2 expression vector was used as a positive control. *TaVIH1/2*, along with *ScVIP1* and empty vector, were transformed individually into wild type and mutant strains by the lithium acetate method with slight modifications. The expression of both TaVIH1-4D and TaVIH2-3B in yeast was confirmed by Western blotting using Anti C-myc antibody (1:1000; raised in mice; Invitrogen, USA). For growth assay, the wild type and mutant *S. cerevisiae* strains carrying different plasmids were allowed to grow overnight in minimal media without uracil. The primary culture was used to re-inoculate fresh media to an OD₆₀₀ of 0.1

and grow until the culture attained an optical density of 0.6–0.8. The cell cultures were then adjusted to O.D of 1 and further serially diluted to the final concentrations of 1:10, 1:100, and 1:1000. Ten microliters each of these cell suspensions was used for spotting on SD(-Ura) plates containing 2% galactose, 1% raffinose, and varying concentrations of 6-azauracil (0, 2.5, and 5 mM). The colony plates were incubated at 30 °C, and pictures were taken after 4 days.

Protein expression of wheat VIH1 and VIH2, in vitro kinase assays, PAGE analysis, and MADLI-ToF analysis

The TaVIH1-KD and TaVIH2-KD were cloned in pET-28a and expressed in *E. coli* BL21 cells using 0.5 mM IPTG and purified in lysis buffer having pH 7.4 containing 50 mM sodium phosphate, 300 mM NaCl, and protein inhibitor cocktail. Post sonication and centrifugation purification was done on the Cobalt resin affinity chromatography column (Thermo Fisher Scientific, Waltham, MA, USA). After column saturation overnight at 4 °C, it was washed with buffer containing 7.5 mM imidazole and subsequently eluted with buffer containing 100 mM EDTA. The eluate was pooled and concentrated using a concentrator having a molecular weight cut-off of 10 kDa by spinning at conditions mentioned in the vivaspin concentrator's manual. The concentrated enzyme preparation was washed thrice with sodium phosphate buffer and finally concentrated in Tris-HCl buffer, pH 7.4. Purified proteins were analyzed by western blotting with mouse anti-HIS primary antibody and goat anti-mouse secondary antibody [HRP IgG (H + L): 1:5000 dilutions; Invitrogen].

Kinase assays were performed using the ADP-Glo™ Max Assay kit (Promega, USA) according to the manufacturer's guidelines. This kit utilizes the luminescence-based test for ADP quantification as a measure of kinase activity. We prepared InsP₇ by using 100 ng of mouse IP6K1 (mIP6K1) recombinant protein along with 100 μM of InsP₆ (Sigma, USA) in a buffer containing 20 mM HEPES (pH 7.5), 5 mM MgCl₂, 10 mM ATP, and 1 mM DTT for 3 h at 28 °C. The resultant product was first resolved by TBE-PAGE gel and then eluted from the gel as described earlier [57] and was used for the reaction. The concentration of the eluted InsP₇ was measured with ImageJ software by comparing with varying InsP₆ concentrations in the TBE-PAGE gels [57]. For ADP-Glo™ Max Assay kit 50 ng of respective protein (VIH1 and VIH2) and 300 nM InsP₇ and 1 μM of ATP was used, and the assay was conducted by following the manufacturer's guidelines. Luminescence was measured 1 h after adding the ADP-Glo™ Max Detection Reagent, using SpectraMax M5e plate reader (Molecular Devices, USA).

For resolving the InsPx species generated by TaVIH1 and TaVIH2, separate kinase assays were performed in 20 mM HEPES (pH 7.5), 5 mM MgCl₂, 10 mM ATP, 100 μM InsP₇, and 1 mM DTT and incubated along with 30 ng of respective proteins in a total volume of 100 μL. ScVIP1 was taken as a control for the reaction. These reactions were incubated at 28 °C for 1, 2, or 9 h. The reaction products were separated by TBE-PAGE and visualized by Toluidine Blue staining. All the inositol polyphosphates were resolved using 18 cm gel using 33.3% polyacrylamide gel in Tris-borate EDTA, as mentioned earlier [28]. These gels were pre-run for 75 min at 300 volts, and the samples were mixed with dye (10 mM Tris-HCl, pH 7.0; 1 mM EDTA; 30% glycerol; 0.08% Orange G) and loaded. Gels were run at 5–6 mA overnight at 4 °C until the Orange G dye front reached 6 cm from the bottom of the gel. Bands were subsequently visualized by Toluidine Blue (0.1% w/v) stain. TBE-PAGE gel-purified products of TaVIH reaction were used for Matrix-assisted laser desorption-Time Of flight Mass Spectrometry analysis (MALDI-ToF-MS). MALDI-ToF-MS was performed from gel extract solutions which were pipetted on an α-Cyano-4-hydroxycinnamic acid (≥ 98%, Sigma) prepared on a stainless steel plate (0.5 μL of a 10 mg/mL ACN/H₂O 1:1 solution). Negative ionization mode was used for acquiring spectra on a spectrometer (AB SCIEX TOF/TOF™ 5800; equipped with a 337-nm laser) operating in the linear mode.

Cloning of VIH promoter, cDNA, and Arabidopsis transformation

For promoter, ~ 2000 bp fragments upstream of the start codon were PCR amplified from genomic DNA. The cloned DNA fragments (in pJET1.2) were sequenced, confirmed, and inserted into pCAMBIA1391z, a promoter-less binary vector containing GUS reporter gene to generate *TaVIHpromoter: GUS* in pCAMBIA1391z. For *VIH2-3B* cDNA (3117 bp) fused C-terminal His tag, site-directed cloning was done at *Spe*I generated site in pCAMBIA1302 (pCAMBIA1302: *TaVIH*-His). These generated transcription units were introduced into *Arabidopsis* seedlings, or T-DNA insertion lines of *vih2-3* (SAIL_165_F12), *vih2-4* (GK-080A07) mutant using *Agrobacterium tumefaciens* (GV3101) mediated transformation by floral dip method (Zhang, Henriques, Lin, Niu & Chua 2006). Multiple (7–10) independent transformants were screened on 0.5× MS media containing 30 mg/L hygromycin and 0.8% agar. The transformed seedlings with long hypocotyls and green expanded leaves at a 4-leaf stage were separated from the non-transformed seedlings and transferred to the soil after about 3 weeks. Similarly, T₁ and T₂ generation seeds were also selected and allowed to grow till maturity. The transgenic seedlings were

confirmed for the presence of recombinant cassette using PCR-based approach. The transgenic lines harboring empty pCAMBIA1391Z or pCAMBIA1302 vector was used as a respective negative control. The PCR-positive lines were further used for functional characterization. In addition, the promoter sequences of *TaVIH* genes were analyzed for the presence of cis-regulatory elements using the PLANTCARE database (<http://bioinformatics.psb.ugent.be/webtools/plantcare/>).

GUS reporter assays and characterization of transgenic lines in *Arabidopsis*

For promoter analysis, the seeds of PCR-positive lines were surface sterilized and grown on 0.5× MS (Murashige and Skoog media) agar plates containing 30 mg/L Hygromycin B for 15 days before they were subjected to various abiotic stress and hormonal treatments. For dehydration stress, the seedlings were air-dried by placing them on Whatman filter paper for 1 h. Exposure to ABA (100 μM), GA₃ (20 μM), and drought-mimic (20% and 30% PEG) were given by placing the seedlings on filter paper impregnated with 0.5× MS solution containing the respective chemical for 24 h. For Pi starvation, seedlings were allowed to grow on MS agar plates without KH₂PO₄ for 96 h. Histochemical staining of seedlings after respective treatments were performed by incubated overnight in GUS staining solution (Jefferson 1987) with 2 mM X-Gluc (5-bromo-4-chloro-3-indolyl-beta-D-glucuronic acid, HiMedia, India) at 37 °C in a 48-well microplate containing about ten seedlings/well. Chlorophyll was removed from tissues by dipping in 90% ethanol. The staining was visualized and photographed under Leica DFC295 stereomicroscope (Wetzlar, Germany) at a magnification of × 63. MS solution without any chemical served as a control.

For characterization of transgenic line parameters such as rosette area, the number of leaves, leaf size, length of central root axis, and number of shoots (primary and secondary). Four independent confirmed homozygous transgenic lines were used for this study. Each parameter was calculated using three experimental replicates, each consisting of twelve plants. For drought-mimic stress experiments, 3-day-old seedlings of transgenic and control pre-grown on 0.5× MS were transferred to 0.5× MS plates consisting of either 125- or 100-mM mannitol or 5 or 10% glycerol. Ten seedlings were used, and the experiments were repeated three times with similar phenotypes. For control, seedlings continued to grow on ½ MS plates. Root lengths were measured, graphs were plotted (using three experimental replicates), and pictures were taken after 9 days of growth. The relative water loss % was calculated of twenty-five leaves per five plants with a similar developmental stage for each of the transgenic lines, and control plants were subjected to incubation

(27 °C) for the period of 8 h. The fresh weight of the detached leaf was taken and continued for the measurements every 2 h. The experiment was repeated twice for similar observations. The leaf relative water content (RWC) measurement was performed as mentioned earlier [41]. The value for each treatment was calculated by using the standard formula $RWC (\%) = [(FW - DW) / (TW - DW)] \times 100$ with FW is fresh weight, DW is dry weight, and TW is turgor weight. For performing these experiments, leaves of equal sizes were detached from 24-day-old transgenic lines and control *Arabidopsis* and weighed immediately (FW). The leaves were submerged in deionized water for 24 h. After incubation, the leaves were blotted dry, and their weight was determined (TW). To measure their DW, they were oven-dried (at 65 °C) for 24 h. The experiments were performed with at least three experimental replicates, each consisting of five to six plants.

For drought response, the seedlings were grown in a symmetrical box with demarcated sections for each seedling. The seedlings were inter-rooted so that they are exposed to similar soil moisture conditions. The 7-day-old seedlings of *Arabidopsis* were subjected to drought (water withholding) conditions for the period of 14 days. After the drought period, the seedlings were re-watered, and observations were made after 4 and 7 days. Post this, the plants were observed, and % survival rates were calculated.

RNAseq profiling

Col-0(Ev) and overexpressing *TaVIH2-3B* *Arabidopsis* (#Line4 and 6) seedlings were grown for 25 days. Total RNA was extracted from three independent biological replicates for each genotype using RNeasy Plant Mini Kits (Qiagen, CA). Genomic DNA contamination was removed by digestion with Turbo DNase (BioRad, CA). RNA quantity was checked by Bioanalyzer for quality control (RIN > 8). Library construction and sequencing were performed by Eurofins, Bangalore, India, using pair-end library preparation. About 9.5 to 13.8 million raw reads were obtained for each sample. Raw reads were processed to filter out the adapter, and low-quality (QV < 20) reads using trimomatic v0.39 [58]. The reads were then pseudo-aligned against the reference transcriptome (Ensembl release 48) using Kallisto v0.46.2 [59]. The obtained raw abundances were summarized to gene-level expression counts using tximport and imported to DESeq2 [60, 61] for differential expression (DE) analysis in R. The obtained log₂ fold change (LFC) values were further processed using apeglm package to reduce noise [26]. Genes with $1 > LFC < -1$ and $p_{adj} < 0.05$ were considered significantly DE. The expression correlation across lines and within replicates was analyzed using principal component analysis (PCA) in

ggplot2 [62]. The data have been deposited in the NCBI as a Bioproject ID PRJNA685929.

GC-MS analysis of Arabidopsis cell-wall polysaccharides and ABA measurement

Extraction of cell-wall components was performed as described earlier with minor modification as depicted in the flowchart as Additional file 14 : Fig. S10 [63]. Since such chemical analysis requires relatively large amounts of samples, pools from 3 to 5 independent plants (for each of the three biological replicates) of the respective lines expressing wheat VIH2-3B were used for chemical analysis. Briefly, 5 g (fresh weight) of shoots from respective lines and control at similar developmental stages (25 days old) was crushed to a fine powder and processed further. The derived pellet was used to extract arabinoxylan (AX) and cellulose, whereas the supernatant was used to extract arabinogalactan (AG). The extractions were checked with iodine solution to make sure that they are free of starch interference. The compositional analysis of the extracted AG, AX, and Cellulose was determined by preparing their alditol derivatives and process for gas chromatography-mass spectrometry (GC-MS) analysis as described [64, 65]. Two microliters of samples was introduced in the splitless injection mode in DB-5 (60 m × 0.25 mm, 1 μm film thickness, Agilent, CA) using helium as a carrier gas. The alditol acetate derivative was separated using the following temperature gradient: 80 °C for 2 min, 80–170 °C at 30 °C/min, 170–240 °C at 4 °C/min, 240 °C held for 30 min and the samples were ionized by electrons impact at 70 eV. ABA was measured using plant hormone abscisic acid (ABA) ELISA kit (Real Gene, Germany). Twenty-five-day-old plant leaves were used for the measurement of the ABA content. One gram of fresh weight from eight plants for each line was used for extractions. The experiments were repeated with at least three independent extractions, and concentration was calculated using standard graphs as per the manual instructions. Standard graph and test samples were plotted using a log of concentration, and color development for each line was measured at 430 nm (Additional file 15 : Fig. S11A and B).

Abbreviations

ADP: Adenosine diphosphate; AG: Arabinogalactan; ATP: Adenosine triphosphate; AX: Arabinoxylan; CYP: Cytochrome P450; DREB: Dehydration response element-binding; DTT: Dithiothreitol; EDTA: Ethylenediaminetetraacetic acid; GA₃: Gibberellic acid; GUS: β-glucuronidase; InsPs: Inositol phosphate; InsP₆: *myo*-inositol-hexakisphosphate, phytic acid; IWGSC: International wheat genome sequencing consortium; KD: Kinase domain; NCED's: 9-*cis*-epoxycarotenoid dioxygenase; IP6Ks: Inositol hexakisphosphate kinases; IPTG: Isopropyl β-D-1-thiogalactopyranosid; ITPKinase: Inositol 1,3,4 trisphosphate 5/6 kinase; PAGE: Polyacrylamide gel electrophoresis; PP-InsPs: Inositol pyrophosphates; PP-IP5Kinase: Diphosphopentakisphosphate kinase; Pi: Phosphate; RLU: Relative luminescence units; RWC: Relative water content; SD: Standard

deviation; TBE: Tris-borate EDTA buffer; TBS: Tris buffered saline; TBST: Tris buffered saline tween; WT: Wild type; YPD: Yeast extract peptone dextrose

Supplementary Information

The online version contains supplementary material available at <https://doi.org/10.1186/s12915-021-01198-8>.

Additional file 1: Fig. S1: Kyte-Doolittle Hydropathy plots and conserved domains of wheat VIH proteins. (A) Kyte-Doolittle hydropathy plots with the positive values indicating the hydrophobic domains and negative values represent hydrophilic regions of the amino acid residues. The hydropathy profile for proteins was calculated according to Kyte and Doolittle, 1982. (B) Schematic representation of domain architecture of TaVIHs deduced from CDD database: light gray rectangles indicate ATP Grasp/RimK Kinase domain and dark gray colored hexagon corresponds to Histidine Phosphatase superfamily.

Additional file 2: Table S1: List of *TaVIH* genes with computed physical and chemical parameters. The molecular weight and isoelectric point prediction were done using ExPASy ProtParam tool (<https://web.expasy.org/protparam/>). The sub-cellular localization prediction was done using WoLF PSORT prediction tool (<http://www.genscript.com/wolf-psort.html>). RefSeq v1.1 for wheat Ensembl Plants was used for gene ID.

Additional file 3: Fig. S2: Multiple Sequence Alignment (MSA) of different VIH/*Vip* protein sequences (TaVIH1, TaVIH2, AtVIH1, AtVIH2 and ScVip1). The red sequence shows high conservation of the amino acids. The single green line indicates rimK/ATP-grasp kinase domain, and the double green line indicates Histidine Phosphatase Domains (HAPs).

Additional file 4: Fig. S3: Yeast complementation assays of wheat VIHs. (A) Total protein was extracted from yeast cell transformed with TaVIH1-4D (C-myc tag) and TaVIH2-3B (C-myc tag) and Western analysis was done (left panel). Representative image of spotting assay performed on SD-Ura plates containing 1% raffinose, 2% galactose and supplemented with 0, 2.5 and 5 mM of 6-azauracil (right panel). The wild type BY4741 and *vip1Δ* strains were transformed with respective constructs using Li-acetate method. Representative images were taken 4 days after the spotting assay was performed. Similar results were obtained with three independent repeats. (B) Filamentous growth assays were observed for wild type yeast (WT), yeast mutant- *vip1Δ* with empty pYES2 (*vip1Δ*) and *TaVIH2-3B* complementation in *vip1Δ*- (*TaVIH2-3B+ Δvip1*). Pictures were taken 20 days post-incubation.

Additional file 5: Fig. S4: Protein purification and western analysis of wheat TaVIH1-KD and TaVIH2-KD. The molecular weight is around 40 kDa. Both the VIH proteins (VIH1 and VIH2) were expressed and purified as mentioned in the Methods section, and the expression was confirmed by the Western analysis using His-antibody.

Additional file 6: Fig. S5: (A) PAGE gel (33%) analysis of mIP6K1 generated product by staining with Toluidine Blue. Substrate InsP₆ without and with ATP (2.5, 5 and 10 mM) was used as a control. The product InsP₇ was generated using mIP6K1 and InsP₆ as a substrate (last lane). (B) The InsP₇ generated by mIP6K1 was eluted from gel and MS analysis was done which indicated a signal at m/z of 740.3 that correspond to mass of InsP₇ and matches with the expected generated species. Indicated by arrow. (C) The kinase reactions were performed using 30 ng of TaVIH1-KD, and TaVIH2-KD purified proteins for 9 hr at 28° C. (D) MALDI-ToF MS analysis of synthesized InsP₈ for TaVIH2-3B KD. MS analysis indicated a significant signal at m/z of 820.47 that correspond to the mass of InsP₈. Indicated by arrow.

Additional file 7: Fig. S6: Hormonal and abiotic stress response of *TaVIH* genes promoter. (A) Cis-element analysis of VIH1 and VIH2 promoters (~ 1 kb) Multiple stress related domains are represented in a schematic form. (B) Representative images for histochemical GUS assay performed against different stresses for promTaVIH1:GUS and promTaVIH2:GUS transgenic lines raised in *Arabidopsis thaliana* Col-0 background. Two-week-old seedlings selected positive against hygromycin selection on 0.5XMS agar plates were subjected to respective treatments: drought (20% PEG), dehydration (1 hr air drying), ABA (100 μM), GA₃ (20 μM) and Pi-deficiency (0.5X MS medias without KH₂PO₄). Seedlings with or without

treatment (control) were stained overnight in GUS staining solution and photographed using Leica stereomicroscope at 6.3X magnification.

Additional file 8: Fig. S7: RNAseq analysis of transgenic Arabidopsis. (A) PCA analysis of the RNAseq for control (Col-0 (Ev)) and two transgenic Arabidopsis lines. (B) Map man analysis of the genes those are consistently represented in the two transgenic Arabidopsis lines with overexpressing TaVH2-3B.

Additional file 9: Table S2: List of genes up- and down-regulated in #line4 (Sheets1,2) and line6 (Sheets3,4) w.r.t. Col-0(Ev) lines. DEGs were obtained using the Kallisto-DESeq2 pipeline; genes with LFC > 1 in either direction and padj < 0.05 were considered to be differentially regulated.

Additional file 10: Fig. S8: qRT-PCR validation of selected genes from the Col-0(Ev), #Line4 and #Line6. A total of 2 µg of RNA (DNA free) was used for cDNA synthesis and qRT-PCR was performed using gene specific primers (Supplementary Table S4). C_t values were normalized against wheat *ARF1* as an internal control.

Additional file 11: Table S3: List of drought responsive genes that are differentially regulated in #line4 (Sheet1), #line6 (Sheet2), and differentially regulated in both #line4 and line6 (Sheet3). Drought responsive genes at 10 days of drought stress w.r.t. Control plants were extracted from the SRA RNAseq dataset (SRP075287) using Cufflinks pipeline. Genes with 1 > LFC < -1 were considered to be drought responsive.

Additional file 12: Fig. S9: Expression patterns of *TaVH* gene homoeologous in different tissues and stress conditions. RNAseq datasets of (A) Tissues and developmental stages (B) Abiotic (phosphate starvation, heat and drought stress) and (C) Biotic stress conditions were used. The expression values were obtained from expVIP database in the form of TPM values and ratios of stressed to control condition were used to generate heatmaps using MeV software. Green and red colors represent down-regulation and up-regulation of the genes in the specific stresses, as shown by the color bar.

Additional file 13: Table S4: List of primers used for this study.

Additional file 14: Fig. S10: Flow representation of the preparation and extraction of polysaccharides (Arabinogalactans, Arabinoxylans and Cellulose) from the shoots of *Arabidopsis*.

Additional file 15: Fig. S11: Standard graph for ABA measurement in plant leaves samples. (A) Y-axis indicates Log of concentration and X-axis indicates the optical density. Data was linearised by plotting the log of the target antigen concentrations versus the log of the OD and the best fit line was determined by regression analysis. (B) Panel showing the color development for the quantitation of the ABA in different leaf samples, OD was taken at 420 nm.

Acknowledgements

Authors thank Executive Director for facilities and support. Part of this work was also supported by the NABI-CORE grant to AKP. MK thanks UGC-CSIR for her research scholarship. Thanks to Dr Gabriel Schaff for sharing the *Arabidopsis vih2-3* and *vih2-4* T-DNA insertion mutant. AS thanks DBT for the SRF fellowship. DBT-eLibrary Consortium (DeLCON) is acknowledged for providing timely support and access to e-resources for this work. We thank Kaushal K. Bhati for providing suggestions for the manuscript.

Authors' contributions

AS, AKP, RB, PP, MK, HR, and VR wrote the text and drafted the figures; AS, SK, AKP, MK, KM, RB, SG, and VK designed and conducted the establishment experiments; GK, AKP, and AS conducted the RNAseq experiments and analyzed the data. AS, MK, and SS performed reporter assays and transgenic related work; AS performed PAGE assays, and RB and SG assisted in the analysis of inositol polyphosphates by PAGE. AKP acquired the funding from the extramural agency. All authors read and approved the final manuscript.

Author's information

Twitter handle: @wheat_biology (Ajay K Pandey)

Funding

This study was supported by the Department of Biotechnology, Basic Plant Biology Grant to AKP [BT/PR/12432/BPA/118/35/2014].

Availability of data and materials

All data generated or analyzed during this study are included in this published article, supplementary information files, and publicly available repositories. The resources, including plasmids, constructs, and transgenic *Arabidopsis* seeds, will be available upon reasonable request. The source of RNAseq data used in the current study is SRA: SRP075287.

Declarations

Ethics approval and consent to participate

Not applicable.

Consent for publication

Not applicable.

Competing interests

The authors declare that they have no competing interests.

Author details

¹National Agri-Food Biotechnology Institute (Department of Biotechnology), Sector 81, Knowledge City, S.A.S. Nagar, Mohali-140306, Punjab, India. ²Regional Centre for Biotechnology, Faridabad - 121001 Haryana (NCR), Delhi, India. ³Laboratory of Cell Signalling, Centre for DNA Fingerprinting and Diagnostics, Hyderabad 500039, India. ⁴Graduate Studies, Manipal Academy of Higher Education, Manipal 576104, India. ⁵Department of Biological Sciences, Indian Institute of Education and Research, Mohali 140306, India. ⁶Department of Plant, Soil, and Microbial Sciences, Michigan State University, East Lansing, MI 48824, USA. ⁷Plant Resilience Institute, Michigan State University, East Lansing, MI 48824, USA.

Received: 26 August 2021 Accepted: 22 November 2021

Published online: 11 December 2021

References

- Irvine RF. Inositol evolution - towards turtle domination? *J Physiol.* 2005; 566(Pt 2):295–300. <https://doi.org/10.1113/jphysiol.2005.087387>.
- Tsui MM, York JD. Roles of inositol phosphates and inositol pyrophosphates in development, cell signaling and nuclear processes. *Adv Enzyme Regul.* 2010;50(1):324–37. <https://doi.org/10.1016/j.advenzreg.2009.12.002>.
- Saiardi A, Erdjument-Bromage H, Snowman AM, Tempst P, Snyder SH. Synthesis of diphosphoinositol pentakisphosphate by a newly identified family of higher inositol polyphosphate kinases. *Curr Biol.* 1999;9(22):1323–6. [https://doi.org/10.1016/S0960-9822\(00\)80055-X](https://doi.org/10.1016/S0960-9822(00)80055-X).
- Saiardi A, Nagata E, Luo HR, Snowman AM, Snyder SH. Identification and characterization of a novel inositol hexakisphosphate kinase. *J Biol Chem.* 2001;276(42):39179–85. <https://doi.org/10.1074/jbc.M106842200>.
- Mulugu S, Bai W, Fridy P, Bastidas R, Otto J, Dollins D, et al. A conserved family of enzymes that phosphorylate inositol hexakisphosphate. *Science.* 2007;316(5821):106–9. <https://doi.org/10.1126/science.1139099>.
- Drašković P, Saiardi A, Bhandari R, Burton A, Ilc G, Kovačević M, et al. Inositol hexakisphosphate kinase products contain diphosphate and triphosphate groups. *Chem Biol.* 2008;15(3):274–86. <https://doi.org/10.1016/j.chembiol.2008.01.011>.
- Laha D, Portela-Torres P, Desfougères Y, Saiardi A. Inositol phosphate kinases in the eukaryote landscape. *Adv Biol Regul.* 2021;79:100782. <https://doi.org/10.1016/j.jbior.2020.100782>.
- Voglmaier SM, Bembenek ME, Kaplin AI, Dormán G, Olszewski JD, Prestwich GD, et al. Purified inositol hexakisphosphate kinase is an ATP synthase: diphosphoinositol pentakisphosphate as a high-energy phosphate donor. *Proc Natl Acad Sci U S A.* 1996;93(9):4305–10. <https://doi.org/10.1073/pnas.93.9.4305>.
- Choi JH, Williams J, Cho J, Falck JR, Shears SB. Purification, sequencing, and molecular identification of a mammalian PP-InsP5 kinase that is activated when cells are exposed to hyperosmotic stress. *J Biol Chem.* 2007;282(42):30763–75. <https://doi.org/10.1074/jbc.M70465200>.
- Fridy PC, Otto JC, Dollins DE, York JD. Cloning and characterization of two human VIP1-like inositol hexakisphosphate and diphosphoinositol pentakisphosphate kinases. *J Biol Chem.* 2007;282(42):30754–62. <https://doi.org/10.1074/jbc.M70465200>.

11. Menniti FS, Oliver KG, Putney JW, Shears SB. Inositol phosphates and cell signaling: new views of InsP5 and InsP6. *Trends Biochem Sci.* 1993;18(2):53–6. [https://doi.org/10.1016/0968-0004\(93\)90053-P](https://doi.org/10.1016/0968-0004(93)90053-P).
12. Stephens L, Radenberg T, Thiel U, Vogel G, Khoo KH, Dell A, et al. The detection, purification, structural characterization, and metabolism of diphosphoinositol pentakisphosphate(s) and bisdiphosphoinositol tetrakisphosphate(s). *J Biol Chem.* 1993;268(6):4009–15. [https://doi.org/10.1016/s0021-9258\(18\)53571-7](https://doi.org/10.1016/s0021-9258(18)53571-7).
13. Luo HR, Saiardi A, Yu H, Nagata E, Ye K, Snyder SH. Inositol pyrophosphates are required for DNA hyperrecombination in protein kinase C1 mutant yeast. *Biochemistry.* 2002;41(8):2509–15. <https://doi.org/10.1021/bi0118153>.
14. Dubois E, Scherens B, Vierendeels F, Ho MMW, Messenguy F, Shears SB. In *Saccharomyces cerevisiae*, the regulation of polyphosphate kinase activity of Kcs1p is required for resistance to salt stress, cell wall integrity, and vacuolar morphogenesis. *J Biol Chem.* 2002;277(26):23755–63. <https://doi.org/10.1074/jbc.m202206200>.
15. Saiardi A. Phosphorylation of proteins by inositol pyrophosphates. *Science* (80-). 2004;306:2101–5. <https://doi.org/10.1126/science.1103344>.
16. Auesukaree C, Tochio H, Shirakawa M, Kaneko Y, Harashima S. Plc1p, Arg82p, and Kcs1p, Enzymes involved in inositol pyrophosphate synthesis, are essential for phosphate regulation and polyphosphate accumulation in *Saccharomyces cerevisiae*. *J Biol Chem.* 2005;280(26):25127–33. <https://doi.org/10.1074/jbc.m414579200>.
17. Wild R, Gerasimaite R, Jung J-Y, Truffault V, Pavlovic I, Schmidt A, et al. Control of eukaryotic phosphate homeostasis by inositol polyphosphate sensor domains. *Science* (80-). 2016;352:986. <https://doi.org/10.1126/science.aad9858>.
18. Norman KL, Shively CA, De La Rocha AJ, Mutlu N, Basu S, Cullen PJ, et al. Inositol polyphosphates regulate and predict yeast pseudohyphal growth phenotypes. *PLoS Genet.* 2018;14(6):e1007493. <https://doi.org/10.1371/journal.pgen.1007493>.
19. Wilson MS, Jessen HJ, Saiardi A. The inositol hexakisphosphate kinases IP6K1 and -2 regulate human cellular phosphate homeostasis, including XPR1-mediated phosphate export. *J Biol Chem.* 2019;294(30):11597–608. <https://doi.org/10.1074/jbc.RA119.007848>.
20. Lemtiri-Chlieh F, MacRobbie EA, Brearley CA. Inositol hexakisphosphate is a physiological signal regulating the K⁺ inward rectifying conductance in guard cells. *Proc Natl Acad Sci U S A.* 2000;97(15):8687–92. <https://doi.org/10.1073/pnas.140217497>.
21. Dorsch JA, Cook A, Young KA, Anderson JM, Bauman AT, Volkman CJ, et al. Seed phosphorus and inositol phosphate phenotype of barley low phytic acid genotypes. *Phytochemistry.* 2003;62(5):691–706. [https://doi.org/10.1016/s0031-9422\(02\)00610-6](https://doi.org/10.1016/s0031-9422(02)00610-6).
22. Laha D, Johnen P, Azevedo C, Dynowski M, Weiß M, Capolicchio S, et al. VIH2 regulates the synthesis of inositol pyrophosphate InsP8 and jasmonate-dependent defenses in *Arabidopsis*. *Plant Cell.* 2015;27(4):1082–97. <https://doi.org/10.1105/tpc.114.135160>.
23. Zhu J, Lau K, Puschmann R, Harmel RK, Zhang Y, Pries V, et al. Two bifunctional inositol pyrophosphate kinases/phosphatases control plant phosphate homeostasis. *Elife.* 2019;8:e43582. <https://doi.org/10.7554/eLife.43582>.
24. Dong J, Ma G, Sui L, Wei M, Satheesh V, Zhang R, et al. Inositol pyrophosphate InsP8 acts as an intracellular phosphate signal in *Arabidopsis*. *Mol Plant.* 2019;12(11):1463–73. <https://doi.org/10.1016/j.molp.2019.08.002>.
25. Desai M, Rangarajan P, Donahue JL, Williams SP, Land ES, Mandal MK, et al. Two inositol hexakisphosphate kinases drive inositol pyrophosphate synthesis in plants. *Plant J.* 2014;80(4):642–53. <https://doi.org/10.1111/tpj.12669>.
26. Zhu A, Ibrahim JG, Love MI. Heavy-tailed prior distributions for sequence count data: removing the noise and preserving large differences. *Bioinformatics.* 2019;35(12):2084–92. <https://doi.org/10.1093/bioinformatics/bty895>.
27. Hura T. Wheat and barley: acclimatization to abiotic and biotic stress. *Int J Mol Sci.* 2020;21(19):7423. <https://doi.org/10.3390/ijms21197423>.
28. Losito O, Szigjarto Z, Resnick AC, Saiardi A. Inositol pyrophosphates and their unique metabolic complexity: analysis by gel electrophoresis. *PLoS One.* 2009;4(5):e5580. <https://doi.org/10.1371/journal.pone.0005580>.
29. Yuan X, Li Y, Liu S, Xia F, Li X, Qi B. Accumulation of eicosapolyenoic acids enhances sensitivity to abscisic acid and mitigates the effects of drought in transgenic *Arabidopsis thaliana*. *J Exp Bot.* 2014;65(6):1637–49. <https://doi.org/10.1093/jxb/eru031>.
30. Chakraborty A, Kim S, Snyder SH. Inositol pyrophosphates as mammalian cell signals. *Sci Signal.* 2011;4:re1. <https://doi.org/10.1126/scisignal.2001958>.
31. Williams SP, Gillaspay GE, Perera IY. Biosynthesis and possible functions of inositol pyrophosphates in plants. *Front Plant Sci.* 2015;6:67. <https://doi.org/10.3389/fpls.2015.00067>.
32. Jadav RS, Chanduri MVL, Sengupta S, Bhandari R. Inositol pyrophosphate synthesis by inositol hexakisphosphate kinase 1 is required for homologous recombination repair. *J Biol Chem.* 2013;288(5):3312–21. <https://doi.org/10.1074/jbc.M112.396556>.
33. Huang S, Sirikhachornkit A, Su X, Faris J, Gill B, Haselkorn R, et al. Genes encoding plastid acetyl-CoA carboxylase and 3-phosphoglycerate kinase of the *Triticum/Aegilops* complex and the evolutionary history of polyploid wheat. *Proc Natl Acad Sci U S A.* 2002;99(12):8133–8. <https://doi.org/10.1073/pnas.072223799>.
34. Dvorak J, Akhunov ED. Tempos of gene locus deletions and duplications and their relationship to recombination rate during diploid and polyploid evolution in the *Aegilops-Triticum* alliance. *Genetics.* 2005;171(1):323–32. <https://doi.org/10.1534/genetics.105.041632>.
35. Adepoju O, Williams SP, Craige B, Cridland CA, Sharpe AK, Brown AM, et al. Inositol trisphosphate kinase and diphosphoinositol pentakisphosphate kinase enzymes constitute the inositol pyrophosphate synthesis pathway in plants. *bioRxiv.* 2019:724914. <https://doi.org/10.1101/724914>.
36. Choi K, Mollapour E, Shears SB. Signal transduction during environmental stress: InsP8 operates within highly restricted contexts. *Cell Signal.* 2005; 17(12):1533–41. <https://doi.org/10.1016/j.cellsig.2005.03.021>.
37. Lee Y-S, Mulugu S, York JD, O'Shea EK. Regulation of a cyclin-CDK-CDK inhibitor complex by inositol pyrophosphates. *Science.* 2007;316(5821):109–12. <https://doi.org/10.1126/science.1139080>.
38. Du H, Liu L, You L, Yang M, He Y, Li X, et al. Characterization of an inositol 1,3,4-trisphosphate 5/6-kinase gene that is essential for drought and salt stress responses in rice. *Plant Mol Biol.* 2011;77(6):547–63. <https://doi.org/10.1007/s11103-011-9830-9>.
39. Marathe A, Krishnan V, Vinutha T, Dahuja A, Jolly M, Sachdev A. Exploring the role of inositol 1,3,4-trisphosphate 5/6 kinase-2 (GmITPK2) as a dehydration and salinity stress regulator in *Glycine max* (L.) Merr. through heterologous expression in *E. coli*. *Plant Physiol Biochem.* 2018;123:331–41. <https://doi.org/10.1016/j.plaphy.2017.12.026>.
40. Daszkowska-Golec A, Szarejko I. The molecular basis of ABA-mediated plant response to drought. *Abiotic Stress - Plant Responses Appl Agric.* 2013. <https://doi.org/10.5772/53128>.
41. Moore JP, Vicré-Gibouin M, Farrant JM, Driouch A. Adaptations of higher plant cell walls to water loss: drought vs desiccation. *Physiol Plant.* 2008; 134(2):237–45. <https://doi.org/10.1111/j.1399-3054.2008.01134.x>.
42. Takahashi F, Kuromori T, Urano K, Yamaguchi-Shinozaki K, Shinozaki K. Drought stress responses and resistance in plants: from cellular responses to long-distance intercellular communication. *Front Plant Sci.* 2020;11:56972. <https://doi.org/10.3389/fpls.2020.56972>.
43. Shinozaki K, Yamaguchi-Shinozaki K. Gene networks involved in drought stress response and tolerance. *J Exp Bot.* 2006;58(2):221–7. <https://doi.org/10.1093/jxb/erl164>.
44. Tenhaken R. Cell wall remodeling under abiotic stress. *Front Plant Sci.* 2015; 5:771. <https://doi.org/10.3389/fpls.2014.00771>.
45. Pandian BA, Sathishraj R, Djanaguiraman M, Prasad PVW, Jugulam M. Role of cytochrome P450 enzymes in plant stress response. *Antioxidants* (Basel, Switzerland). 2020;9:454. <https://doi.org/10.3390/antiox9050454>.
46. Shinozaki K, Yamaguchi-Shinozaki K. Molecular responses to dehydration and low temperature: differences and cross-talk between two stress signaling pathways. *Curr Opin Plant Biol.* 2000;3(3):217–23. [https://doi.org/10.1016/S1369-5266\(00\)80068-0](https://doi.org/10.1016/S1369-5266(00)80068-0).
47. Schroeder JI, Kwak JM, Allen GJ. Guard cell abscisic acid signalling and engineering drought hardiness in plants. *Nature.* 2001;410(6826):327–30. <https://doi.org/10.1038/35066500>.
48. Hwang S-G, Chen H-C, Huang W-Y, Yu-Chun C, Shii C-T, Cheng W-H. Ectopic expression of rice OsNCED3 in *Arabidopsis* increases ABA level and alters leaf morphology. *Plant Sci.* 2010;178(1):12–22. <https://doi.org/10.1016/j.plantsci.2009.09.014>.
49. Qin X, Zeevaart JAD. Overexpression of a 9-cis-epoxycarotenoid dioxygenase gene in *Nicotiana glauca* increases abscisic acid and

- phaseic acid levels and enhances drought tolerance. *Plant Physiol.* 2002; 128(2):544–51. <https://doi.org/10.1104/pp.010663>.
50. Iuchi S, Kobayashi M, Taji T, Naramoto M, Seki M, Kato T, et al. Regulation of drought tolerance by gene manipulation of 9-cis-epoxycarotenoid dioxygenase, a key enzyme in abscisic acid biosynthesis in *Arabidopsis*. *Plant J.* 2001;27(4):325–33. <https://doi.org/10.1046/j.1365-313x.2001.01096.x>.
 51. Klein M, Perfus-Barbeoch L, Frelet A, Gaedeke N, Reinhardt D, Mueller-Roeber B, et al. The plant multidrug resistance ABC transporter AtMRP5 is involved in guard cell hormonal signalling and water use. *Plant J.* 2003; 33(1):119–29. <https://doi.org/10.1046/j.1365-313x.2003.016012.x>.
 52. Wilson MSC, Bulley SJ, Pisani F, Irvine RF, Saiardi A. A novel method for the purification of inositol phosphates from biological samples reveals that no phytate is present in human plasma or urine. *Open Biol.* 2015;5(3):150014. <https://doi.org/10.1098/rsob.150014>.
 53. De Vos M, Denekamp M, Dicke M, Vuylsteke M, Van Loon L, Smeekens SC, et al. The *Arabidopsis thaliana* transcription factor AtMYB102 functions in defense against the insect Herbivore *Pieris rapae*. *Plant Signal Behav.* 2006; 1(6):305–11. <https://doi.org/10.4161/psb.1.6.3512>.
 54. Shukla V, Kaur M, Aggarwal S, Bhati KK, Kaur J, Mantri S, et al. Tissue specific transcript profiling of wheat phosphate transporter genes and its association with phosphate allocation in grains. *Sci Rep.* 2016;6(1):39293. <https://doi.org/10.1038/srep39293>.
 55. Mizianty MJ, Stach W, Chen K, Kedarisetti KD, Disfani FM, Kurgan L. Improved sequence-based prediction of disordered regions with multilayer fusion of multiple information sources. *Bioinformatics.* 2010;26(18):i489–96. <https://doi.org/10.1093/bioinformatics/btq373>.
 56. Livak KJ, Schmittgen TD. Analysis of relative gene expression data using real-time quantitative PCR and the 2^{-ΔΔCT} method. *Methods.* 2001;25(4): 402–8. <https://doi.org/10.1006/meth.2001.1262>.
 57. Loss O, Azevedo C, Szijgyarto Z, Bosch D, Saiardi A. Preparation of quality inositol pyrophosphates. *J Vis Exp.* 2011:e3027. <https://doi.org/10.3791/3027>.
 58. Bolger AM, Lohse M, Usadel B. Trimmomatic: a flexible trimmer for Illumina sequence data. *Bioinformatics.* 2014;30(15):2114–20. <https://doi.org/10.1093/bioinformatics/btu170>.
 59. Bray NL, Pimentel H, Melsted P, Pachter L. Erratum: Near-optimal probabilistic RNA-seq quantification. *Nat Biotechnol.* 2016;34(8):888. <https://doi.org/10.1038/nbt0816-888d>.
 60. Love MI, Huber W, Anders S. Moderated estimation of fold change and dispersion for RNA-seq data with DESeq2. *Genome Biol.* 2014;15(12):550. <https://doi.org/10.1186/s13059-014-0550-8>.
 61. Soneson C, Love MI, Robinson MD. Differential analyses for RNA-seq: transcript-level estimates improve gene-level inferences. *F1000Research.* 2015;4:1521. <https://doi.org/10.12688/f1000research.7563.2>.
 62. Gómez-Rubio V. ggplot2 - Elegant Graphics for Data Analysis (2nd Edition). *J Stat Softw.* 2017;77(Book Review):2. <https://doi.org/10.18637/jss.v077.b02>.
 63. Zablackis E, Huang J, Müller B, Darvill AG, Albersheim P. Characterization of the cell-wall polysaccharides of *Arabidopsis thaliana* leaves. *Plant Physiol.* 1995;107(4):1129–38. <https://doi.org/10.1104/pp.107.4.1129>.
 64. Blakeney AB, Harris PJ, Henry RJ, Stone BA. A simple and rapid preparation of alditol acetates for monosaccharide analysis. *Carbohydr Res.* 1983;113(2): 291–9. [https://doi.org/10.1016/0008-6215\(83\)88244-5](https://doi.org/10.1016/0008-6215(83)88244-5).
 65. Bhagia S, Nunez A, Wyman CE, Kumar R. Robustness of two-step acid hydrolysis procedure for composition analysis of poplar. *Bioresour Technol.* 2016;216:1077–82. <https://doi.org/10.1016/j.biortech.2016.04.138>.

Publisher's Note

Springer Nature remains neutral with regard to jurisdictional claims in published maps and institutional affiliations.

Ready to submit your research? Choose BMC and benefit from:

- fast, convenient online submission
- thorough peer review by experienced researchers in your field
- rapid publication on acceptance
- support for research data, including large and complex data types
- gold Open Access which fosters wider collaboration and increased citations
- maximum visibility for your research: over 100M website views per year

At BMC, research is always in progress.

Learn more biomedcentral.com/submissions

